8-2011

Haptic Tele-operation of Wheeled Mobile Robot and Unmanned Aerial Vehicle over the Internet

Zhiyuan Zuo
zzuo1@utk.edu

To the Graduate Council:

I am submitting herewith a thesis written by Zhiyuan Zuo entitled "Haptic Tele-operation of Wheeled Mobile Robot and Unmanned Aerial Vehicle over the Internet." I have examined the final electronic copy of this thesis for form and content and recommend that it be accepted in partial fulfillment of the requirements for the degree of Master of Science, with a major in Mechanical Engineering.

Dongjun Lee, Major Professor

We have read this thesis and recommend its acceptance:

Xiaopeng Zhao, William R. Hamel

Accepted for the Council:
Dixie L. Thompson

Vice Provost and Dean of the Graduate School

(Original signatures are on file with official student records.)

To the Graduate Council:

I am submitting herewith a thesis written by Zhiyuan Zuo entitled "Haptic Teleoperation of Wheeled Mobile Robot and Unmanned Aerial Vehicle over the Internet." I have examined the final paper copy of this thesis for form and content and recommend that it be accepted in partial fulfillment of the requirements for the degree of Master of Science, with a major in Mechanical Engineering.

_____

Dongjun Lee, Major Professor

We have read this thesis
and recommend its acceptance:

_____

Xiaopeng Zhao

_____

William R. Hamel

Accepted for the Council:

_____

Carolyn R. Hodges

Vice Provost and Dean of the Graduate School

To the Graduate Council:
I am submitting herewith a thesis written by Zhiyuan Zuo entitled "Haptic Teleoperation of Wheeled Mobile Robot and Unmanned Aerial Vehicle over the Internet." I have examined the final electronic copy of this thesis for form and content and recommend that it be accepted in partial fulfillment of the requirements for the degree of Master of Science, with a major in Mechanical Engineering.

Dongjun Lee, Major Professor

We have read this thesis
and recommend its acceptance:

Xiaopeng Zhao

William R. Hamel

Accepted for the Council:

Carolyn R. Hodges

Vice Provost and Dean of the Graduate School

(Original signatures are on file with official student records.)

Haptic Tele-operation of Wheeled Mobile Robot and Unmanned Aerial Vehicle over the Internet

A Thesis Presented for

The Master of Science

Degree

The University of Tennessee, Knoxville

Zhiyuan Zuo

August 2011

To my dear family

Acknowledgements

First, I would like to thank my adviser Dongjun Lee who offers me the opportunity to work on these challenging and interesting projects, who guides me in the new area of study, and who serves as a wonderful example of researcher.

I would also thank Dr. Hamel and Dr. Zhao for being my committee members and providing valuable advice in my research and thesis writing. Also, thank the faculties in Engineering/Math School who taught me those interesting and useful theories.

Thank my friends in the my research lab INRoL: Ke, Daye, Tian and Robert, who helped me a lot in working and study, and who shared with me laugh and knowledge.

Also, thank my family who are watching and thinking of me all the time.

Abstract

Teleoperation of ground/aerial vehicle extends operator's ability (e.g. expertise, strength, mobility) into the remote environment, and haptic feedback enhances the human operator's perception of the slave environment. In my thesis, two cases are studied: wheeled mobile robot (MWR) haptic tele-driving over the Internet and unmanned aerial vehicle (UAV) haptic teleoperation over the Internet. We propose novel control frameworks for both dynamic WMR and kinematic WMR in various tele-driving modes, and for a "mixed" UAV with translational dynamics and attitude kinematics. The recently proposed passive set-position modulation (PSPM) framework is extended to guarantee the passivity and/or stability of the closed-loop system with time-varying/packet-loss in the communication; and proved performance in steady state is shown by theoretical measurements. For UAV teleoperation, we also derive a backstepping trajectory tracking control with robustness analysis. Experimental results for dynamic/kinematic WMR and an indoor quadrotor-type UAV are presented to show the efficacy of the proposed control framework.

Contents

List of Figures

Chapter 1

Introduction

Vehicle teleoperation finds its application in various cases: planet exploration (Schenker et al. (2003)), landscape survey (Valavanis (2007)), transportation and rescue (Nourbakhsh et al. (2005)), material handling (Peshkin and Colgate (1999)), or deep sea exploration (Baiden and Bissiri (2007)). By tele-driving aerial/ground/under water vehicles, human's skill, strength and mobility are extended to the remote environment. Besides, haptic teleoperation enables human to operate by haptic feeling. This enhances environment awareness and improves efficiency, especially when the vehicle is in clustered/dark environment (Lim et al. (2003); Cho et al. (2010); Lamb (1895)). Haptic feedback become more important if the communication bandwidth is restricted or when the task requires awareness of certain mechanical aspect (e.g. pushing force against the object, inertia of the WMR).

Two cases are studied in my research: wheeled mobile robot (WMR) tele-driving (Zuo and Lee (2010)) and quad-rotor type UAV(unmanned aerial vehicle) teleoperation through haptic device over the Internet (Zuo and Lee (2011)).

For WMR tele-driving, we aim to achieve car-driving metaphor, that is, we use one-DOF (degree of freedom) as the gas-pedal to control its linear velocity, while the other-DOF as the wheel to control its heading angle or angular rate. Meanwhile, we want to offer useful haptic feedback indicating the motion of the WMR (e.g.

velocity, heading angle or angular rate) and environment force (e.g. repulsion from obstacles perceived through sensors). For UAV teleoperation, we want to control its translational velocity in the space by 3-DOFs of the haptic device, and to perceive velocity and environment force at the same time. In both cases, we need to cope with the problem of time-varying delay and packet-loss in communication, so that the systems can work properly over the Internet.

It is known that time delay can easily induce bilateral tele-operators to be unstable, and this problem is extensively studied since 1980s. Among these approaches passivity based methods, like scattering based method (Anderson and Spong (1989a)) or wave based method (Niemeyer and Slotine (1991)), have more advantage when dealing with the uncertainties in operator/environment, compared to Leung et al. (1995)'s μ-synthesis or Lawrence (1993)'s performance-oriented method. One the other hand, communication through Internet brings about more challenges, like the instability caused by varying delay and packet-loss. Scattering/Wave based method is modified to deal with varying delay (Chopra et al. (2003); Niemeyer and Slotine (1998) or packet loss (Berestesky et al. (2004a); Hirche and Buss (2004); and some new passivity based methods appeared, e.g. PD-like control (Lee and Spong (2006a); Nuño et al. (2009a)), Passity-Observer/Passivity-Controller(Hannaford and Ryu (2002)) or Passive-Set-Position-Modulation (Lee and Huang (2009b)).

When it comes to tele-operating the mobile robot, more difficulties appear. Instead of positon-position coupling, positon-velocity coupling is required, since the workspace of the master device is bounded while the that of the slave robot is unbounded. The scattering/wave based method , where mechanical power is taken as the power supple, is not suitable to solve this problem. For this, Salcudean et al. (2000) proposed the rate control, yet lacked robust analysis; Lee et al. (2006a) proposed a r-passivity method to achieve stable teleoperation.

Meanwhile some works have been done for vehicle teleoperation. For dynamic WMRs, a passivity-based control design is proposed by Lee et al. (2006b), yet only for the $(q_1, \nu)/(q_2, \phi)$ mode with constant delay assumption. For kinematic haptic

tele-driving, some methods are given by Lee et al. (2002) and Lim et al. (2003), yet the effect of force reflection on the stability is not considered. Another passivity-based method is proposed by Diolaiti and Melchiorri (2002) by introducing a virtual mass on the slave side, yet the effect of communication delay between the virtual mass and the haptic device on the passivity is not analyzed. Communication delay and its associated stability problems are considered by Slawinski et al. (2007) and Elhajj et al. (2001); however, the result by Slawinski et al. (2007) involves only vision feedback but no haptic feedback, and the scheme by Elhajj et al. (2001) divides the continuous operation into events, which may not suitable for continuous-time stability analysis, and its performance may deteriorate when delay is not small (around 300ms). Besides, all of these works, except that of Lee et al. (2006b), consider only the kinematic WMRs, thus, cannot address (often important) mechanical aspects (e.g. force between the environment, inertia of WMR, etc.).

UAV teleoperation also becomes an popular topic recently, Lam et al. (2009) propose an artificial field method suitable for UAV teleoperation, yet the delay in the communication is not considered. Rodríguez-Seda et al. (2010) consider the stability problem using PD-based control (Lee and Spong (2006a)) yet only for position-position coordination with constant time delay. Stramigioli et al. (2010) introduce a virtual vehicle controlled by haptice device and coupled with the actual vehicle, stability of the master and virtual vehicle is guaranteed by using Hamiltonian method, and a controller to couple virtual/actual vehicle is proposed based on the assumption that attitude dynamic is much faster than translational dynamic. The robustness of the controller for coupling is not clear. Blthoff (2010) deal with the stability problem using passive-set-position-modulation (PSPM) method and achieve master-passivity/VPs-stability.

In the thesis, we design frameworks for WMR tele-driving and quad-rotor type UAV teleoperation over the Internet. Stability is guaranteed and performance is measured for the teleoperation system with varying-delay/packet-loss/data-swapping in the communication.

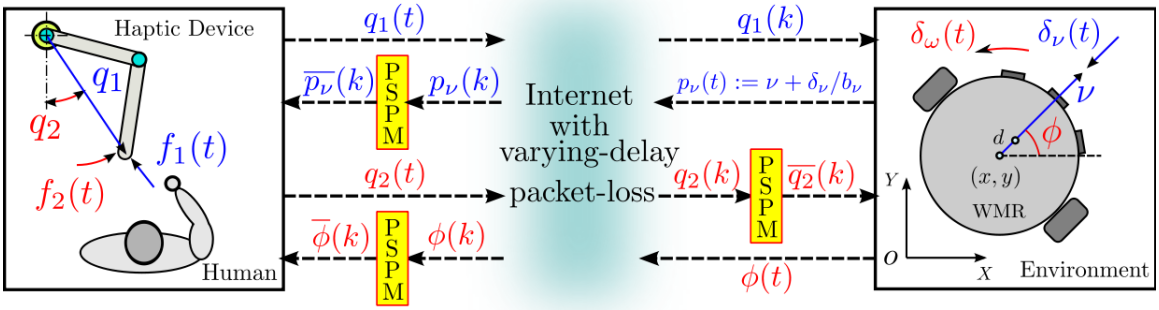

Figure 1.1: Dynamic WMR tele-driving $(q_1, \nu)/(q_2, \phi)$ mode. To achieve *car driving metaphor*, we use q_1 to control WMR's forward motion (ν), and q_2 WMR's turning motion (ϕ or $\dot{\phi}$).

For WMR tele-driving, we also adopt *car driving metaphor* Diolaiti and Melchiorri (2002); Lee et al. (2002, 2006b), as illustrated in Fig. 3.1, we use one-DOF (degree-of-freedom) of the master device (e.g. q_1) to control the WMR's forward velocity ν (i.e. (q_1, ν) tele-driving), while another-DOF (e.g. q_2) the WMR's heading angle ϕ or its rate $\dot{\phi}$ (i.e. (q_2, ϕ) or $(q_2, \dot{\phi})$ tele-driving). By this car driving metaphor, operators can tele-drive the WMR as if they are driving a car, with q_1 and q_2 being used as the gas pedal and the steering wheel, respectively.

For the UAV teleoperation, see Fig. 4.1, we use 3-DOF of the haptic device to control the velocity of the UAV. A virtual point is introduced and simulated in the virtual environment. The virtual point velocity $\dot{p}$ is controlled by the configuration of the hapitc device q, and affected by the repulsion $\frac{\partial \varphi_o^T}{\partial p}$ from the virtual obstacle. Then the actual UAV follows the virtual point through a backstepping controller. The UAV is modeled by a combination of translational dynamics and attitude kinematics on $SE(3)$, with the thrust λ (along one body-fixed frame - e.g. e_3) and the two angular rates ω_1, ω_2 (along the remaining two body-fixed axes - e.g. e_1, e_2) as the control input. This model can be used for many commercially available UAVs, including our laboratory systems, Asctec Hummingbird, only allow us to control their thrust force and angular rates, not their angular torques. This is because, usually, they are

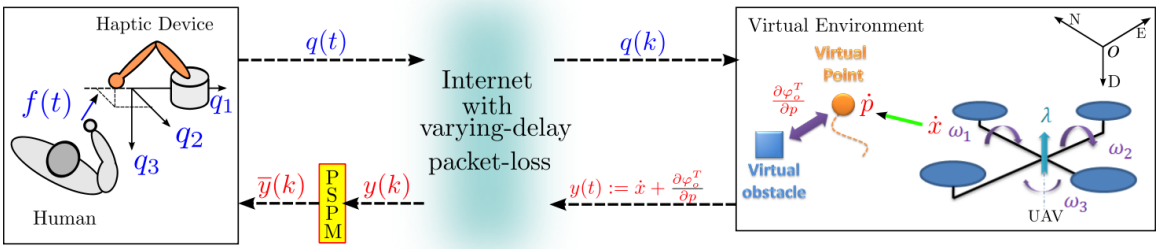

Figure 1.2: UAV teleoperation. The velocity of the virtual point $\dot{p}$ is controlled by the configuration of the hapitc device q, and affected by the repulsion $\frac{\partial \varphi_o^T}{\partial p}$ from the virtual obstacle. The UAV follows the virtual point through a backstepping controller

shipped with some low-level attitude control module already in place. Even if our main focus is on such "mixed" UAVs, we also believe our results as proposed here would also be applicable to many UAVs accepting the angular torques as their inputs, by achieving these desired angular rates, which is very often possible since most of UAVs' attitude dynamics is fully actuated.

In contrast to the case in conventional teleoperation where the workspace for master and slave robot are bounded, here we want to achieve position-to-velocity coupling (e.g. (q_2, ν) for WMR or $(q, \dot{x})$ for UAV). Thus the conventional approach dealing with position-to-position coordination over Internet, like Berestesky et al. (2004b); Nuño et al. (2009b), cannot be readily used. To solve this problem, we utilize the recently proposed passive set-position modulation (PSPM) framework (Lee and Huang (2008); Lee (2008); Lee and Huang (2009a,b), which can modulate set-position signal received from the Internet within the tele-driving control-loop to enforce (closed-loop/hybrid) passivity, even if this set-position signal undergoes varying-delay and packet-loss. Due to the flexibility of PSPM (Lee and Huang (2009b)), we can encode other information, like the value of WMR velocity or virtual environment force, into the set-position signal (e.g. $p_\nu(t)$ in Fig. 3.1 or $y(t)$ in Fig. 4.1) and achieve position-to-velocity coordination and force reflection. Also, compared to other "time-invariant" techniques for delayed-teleoperation (e.g. Anderson and Spong (1989b);

Niemeyer and Slotine (2004); Lee and Spong (2006b)), PSPM selectively triggers the passifying action and substantially improves the performance.

More specifically, we first extend the framework proposed in Lee (2008) for the $(q_1, \nu)/(q_2, \phi)$ tele-driving of the dynamic WMR, by incorporating the scaling of the master-slave power-shuffling. This scaled power-shuffling was motivated by our observation that the human energy, shuffled via the PSPM to drive the WMR, was very often all dissipated by the WMR's large dissipation (e.g. gearbox, tire/ground interaction, etc.). This power-shuffling scaling enables us to virtually scale up the human power, thereby addressing such high dissipation. We also propose the PSPM control frameworks for the $(q_1, \nu)/(q_2, \dot{\phi})$ tele-driving of the dynamic WMR, and for the $(q_1, \nu)/(q_2, \phi)$ and $(q_1, \nu)/(q_2, \dot{\phi})$ tele-driving of the kinematic WMRs. The flexibility of the PSPM allows us to achieve teleoperation of the dynamic/kinematic WMR and UAV, while retaining peculiarity of each tele-driving mode (e.g. usual two-port passivity for dynamic WMR; or a combination of passivity/stability for UAV).

As for the quadrotor-type UAV, numerous control laws available (e.g. Frazzoli et al. (2000); Mahony and Hamel (2004); Castillo et al. (2004); Bouabdallah and Siegwart (2005); Aguiar and Hespanha (2007); Hua et al. (2009)) and some of them utilize backstepping control on $SE(3)$ as we do in this paper (e.g. Frazzoli et al. (2000); Mahony and Hamel (2004); Aguiar and Hespanha (2007)). Yet, derived for the UAVs with the translation and attitude dynamics, these backstepping control laws are not directly applicable to, and also unnecessarily complicated for, such "mixed" UAVs with attitude kinematics (and control inputs $\lambda, \omega_1, \omega_2$). Compared with others, the control law proposed in this thesis possess two advantages: 1) it is *flexible* in the sense that many control laws designed/verified point mass dynamics can be incorporated into our backstepping control framework. 2) it is *transparent* in the sense that its gain tuning can be done much more intuitively, since all of its gain parameters can be interpreted either as parameters of standard second-order dynamics (e.g. damping or spring) or convergence factor of first-order dynamics. For the real implementation,

we also provide robustness analysis for our backstepping control law against mass (or thrust) parameter estimation error and Cartesian disturbance (e.g. wind gust); and show that, as long as they are bounded, the trajectory tracking is still ultimately bounded Khalil (1996).

The rest of the thesis is organized as follows: Chapter 2 presents some preliminary materials about PSPM. Chapter 3 gives the controller design for WMR haptic teledriving and Chapter 4 for UAV haptic teleoperation. The experimental result is shown in Chapter 5.

Chapter 2

Background

2.1 Passive Set-Position Modulation

Consider the following second order robotic system:

$$M(x)\ddot{x} + C(x,\dot{x})\dot{x} = \tau + f \tag{2.1}$$

where $M(x), C(x,\dot{x}) \in \Re^{n\times n}$ are the inertia and Coriolis matrix, with $x, \tau, f \in \Re^n$ being the configuration, control and human/environment force respectively. Suppose we aim to coordinate $x(t)$ with a sequence of discrete signal $y(k) \in \Re^n$, via a local spring coupling with damping injection, that is, for $t \in [t_k, t_{k+1})$,

$$\tau(t) = -B\dot{x}(t) - K(x(t) - y(k)). \tag{2.2}$$

The main problem of this simple coupling is that: due to the switches of $y(k)$, energy in the spring K can jump, accumulate and eventually make this coupling control unstable.

PSPM can passify these spring jumps by watching the energy in the system and selectively modulating the set-position signal from $y(k)$ to $\overline{y}(k)$. To describe PSPM in Algo.1, let us denote the estimate of damping dissipation as $D_{min}(k)$, with $D_{min}(k) \leq$

Algorithm 1 Passive Set-Position Modulation

1: $\bar{y}(0) \Leftarrow x(0),\ E(0) \Leftarrow \bar{E},\ k \Leftarrow 0$
2: **repeat**
3: **if** data $(y, \Delta E_y)$ is received **then**
4: $k \Leftarrow k+1$
5: $y(k) \Leftarrow y,\ \Delta E_y(k) \Leftarrow \Delta E_y$
6: retrieve $x(t_k),\ x_i^{\max}(k-1),\ x_i^{\min}(k-1)$
7: find $\bar{y}(k)$ by solving

$$\min_{\bar{y}(k)} \quad ||y(k) - \bar{y}(k)|| \tag{2.3}$$

$$\text{subj. } E(k) \Leftarrow E(k-1) + \Delta E_y(k) + D_{\min}(k-1) - \Delta \bar{P}(k) \geq 0 \tag{2.4}$$

8: **if** $E(k) > \bar{E}$ **then**
9: $\Delta E_x(k) \Leftarrow E(k) - \bar{E},\ E(k) \Leftarrow \bar{E}$
10: **else**
11: $\Delta E_x(k) \Leftarrow 0$
12: **end if**
13: send $(x(t_k), \Delta E_x(k))$ or discard
14: **end if**
15: **until** termination

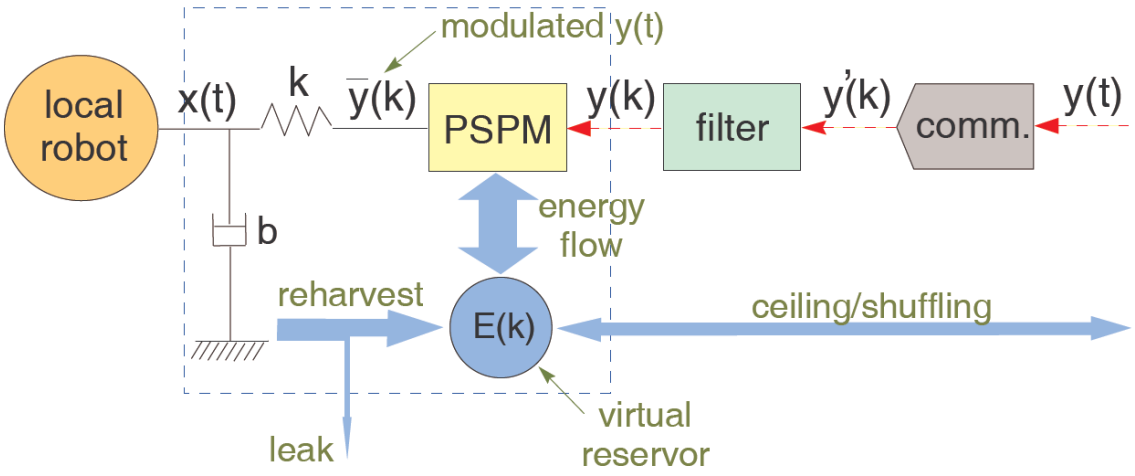

Figure 2.1: Energetics of the passive set-point modulation

$D(k) := \int_{t_k}^{t_{k+1}} ||\dot{x}||_B^2$, and define modulated energy jump $\Delta\overline{P}(k)$ as,

$$\Delta\overline{P}(k) := (1/2)||x(t_k) - \overline{y}(k)||_K^2 - (1/2)||x(t_k^-) - \overline{y}(k-1)||_K^2$$

where $||\star||_K := \sqrt{\star^T K \star}$ and $\overline{y}(k)$ is the modulated version of $y(k)$ via PSPM. PSPM modulates $y(k)$ to $\overline{y}(k)$ in such a way that $\overline{y}(k)$ is as close to $y(k)$ as possible (2.3), while the energy jump $\Delta\overline{P}(k)$ is limited by available energy in the system (2.4). Here the available energy at time t_k is the sum of $E(k-1)$, $\Delta E_y(k)$ and $D_{min}(k-1)$, where $E(k-1)$ is the energy left in the energy reservoir, $\Delta E_y(k)$ the shuffled energy from peer PSPM, and $D_{min}(k-1)$ a (substantial) portion of recycled damping dissipation of B during $[t_{k-1}, t_k)$. Step 8-13 in Algorithm 1 define energy ceiling/shuffling, where the energy reservoir $E(k)$ is ceiled by $\overline{E}$, and the excessive energy $\Delta E_x(k)$ is returned to the peer PSPM or discarded if no peer exists. See Fig. 2.1 for energetics of PSPM.

Using the modified control input (i.e. $\tau = -B\dot{x} - K(x - \overline{y}(k))$) for system (2.1), we have the following inequality, which will be used later in this paper, $\forall T \in [t_N, t_{N+1})$

$$\begin{aligned}
\int_0^T f^T \dot{x} dt &= V(T) - V(0) \\
&\quad + \sum_{k=0}^{N-1} D(k) - \sum_{k=1}^{N} \Delta\overline{P}(k) + \int_{t_N}^{T} ||\dot{x}||_B^2 \\
&\geq V(T) - V(0) + \sum_{k=1}^{N} [D_{min}(k-1) - \Delta\overline{P}(k)] \\
&= V(T) - V(0) + E(N) - E(0) \\
&\quad + \sum_{k=1}^{N} \Delta E_x(k) - \sum_{k=1}^{N} \Delta E_y(k)
\end{aligned} \tag{2.5}$$

where $V(T) := (1/2)||\dot{x}||_{M(x)}^2 + (1/2)||x(T) - \overline{y}(N)||_K^2$, and the last equality is due to

$$D_{min}(k-1) - \Delta\overline{P}(k) = E(k) - E(k-1) + \Delta E_x(k) - \Delta E_y(k) \tag{2.6}$$

which can be obtained through step 7-12 in Algo.1.

Chapter 3

Wheeled mobile robot tele-driving over the internet

3.1 Problem Setting of WMR Tele-Driving

We use a differential wheeled robot, see Fig. 3.1, as the slave wheeled mobile robot (WMR). Denote its 3-DOF configuration by $(x, y, \phi) \in SE(2)$, with $(x, y) \in E(2)$ being the WMR geometric center position and $\phi \in S$ the heading angle w.r.t. the global frame (O, X, Y), then the no-slip constraint can be written as:

$$\frac{d}{dt}\begin{pmatrix} x \\ y \\ \phi \end{pmatrix} = \begin{bmatrix} \cos\phi & 0 \\ \sin\phi & 0 \\ 0 & 1 \end{bmatrix} \begin{pmatrix} \nu \\ \omega \end{pmatrix} \tag{3.1}$$

where $\nu \in \Re$ is the forward velocity of (x, y) and $\omega := \dot{\phi}$ is the angular velocity. When the driven wheels accept torque as the input, WMR's dynamics can be written as Lee (2007):

$$\begin{bmatrix} m & 0 \\ 0 & I \end{bmatrix} \begin{pmatrix} \dot{\nu} \\ \dot{\omega} \end{pmatrix} + \begin{bmatrix} 0 & -md\dot{\phi} \\ md\dot{\phi} & 0 \end{bmatrix} \begin{pmatrix} \nu \\ \omega \end{pmatrix} = u + \delta \tag{3.2}$$

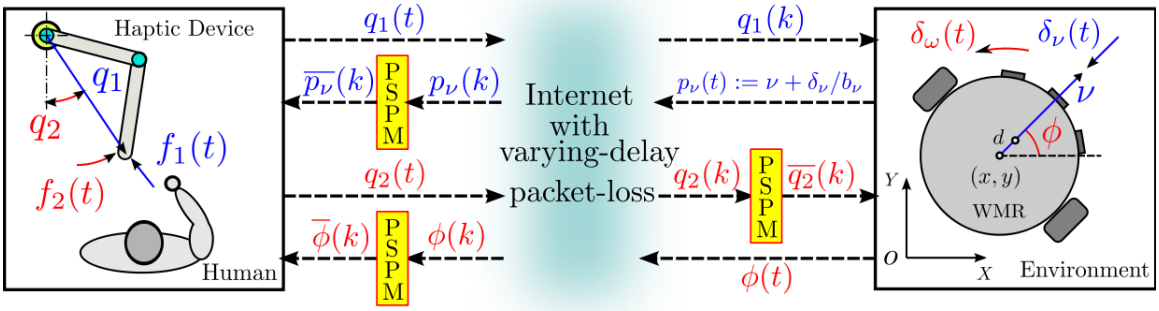

Figure 3.1: Dynamic WMR tele-driving $(q_1, \nu)/(q_2, \phi)$ mode. To achieve *car driving metaphor*, we use q_1 to control WMR's forward motion (ν), and q_2 WMR's turning motion (ϕ or $\dot{\phi}$).

where $I := I_c + md^2$ with $m, I_c > 0$ being the mass and moment of inertia w.r.t. the center of mass; d is the distance between the geometric center and the mass center; and $u = [u_\nu, u_\omega]^T$, $\delta = [\delta_\nu, \delta_\omega]^T$ are the control and the external force/torque. For simplicity, in this paper, we assume $d \approx 0$, or we can cancel out the Coriolis terms in (3.2) via a certain local control. Then, its reduced dynamics can be given by:

$$\begin{bmatrix} m & 0 \\ 0 & I \end{bmatrix} \begin{pmatrix} \dot{\nu} \\ \dot{\omega} \end{pmatrix} = u + \delta. \tag{3.3}$$

We call the above WMR described by (3.1) and (3.3) **dynamic WMR**. On the other hand, many commercial WMRs (e.g. Pioneer DX-3 or e-puck) only accept ν, ω as the input signal, that is, its evolution is given by (3.1) and the following input equation:

$$\begin{pmatrix} \nu \\ \omega \end{pmatrix} = u \tag{3.4}$$

where $u = [u_\nu, u_\omega]^T$ is the input signal. If WMR can be written by (3.1) and (3.4), we call it **kinematic WMR**.

We want to achieve *car-driving metaphor* Diolaiti and Melchiorri (2002); Lee et al. (2002, 2006b): master's one-DOF serves as the gas-pedal to command ν, while the other-DOF as the steering-wheel to command ϕ (or $\dot{\phi}$). For this, we use the following 2-DOF linear master-joystick:

$$h_1\ddot{q}_1 = c_1 + f_1, \quad h_2\ddot{q}_2 = c_2 + f_2 \tag{3.5}$$

where $h_i, q_i, c_i, f_i \in \Re$ are the mass, configuration, control, and human force.

In this paper, we assume that suitable motion/power scaling factors, as in Lee and Li (2003, 2005), are embedded in equations (3.1)-(3.5) to solve the mismatch in the scale between the master device and WMR. We want to coordinate q_1 with ν and q_2 with ϕ (or $\dot{\phi}$) for both dynamic and kinematic WMR. Then, we can think of the four modes of tele-driving: 1) dynamic WMR $(q_1, \nu)/(q_2, \phi)$ tele-driving; 2) dynamic WMR $(q_1, \nu)/(q_2, \dot{\phi})$ tele-driving; 3) kinematic WMR $(q_1, \nu)/(q_2, \phi)$ tele-driving; and 4) kinematic WMR $(q_1, \nu)/(q_2, \dot{\phi})$ tele-driving. For each of them, we design PSPM-based tele-driving control laws. Before doing that, we briefly review the PSPM framework.

3.2 Dynamic WMR Tele-Driving Control

3.2.1 $(q_1, \nu)/(q_2, \phi)$ Tele-Driving

We first consider the $(q_1, \nu)/(q_2, \phi)$ tele-driving of the dynamic WMR. For this, we extend the result of Lee (2008) by incorporating the scaling ρ_s of the master-slave PSPM power shuffling. This turns out to be crucial if the WMR has substantial dissipation, for which, if not scaled up, the virtually shuffled human power via PSPM is simply all dissipated, thus, cannot drive the WMR. Although our derivation here is similar to that of Lee (2008), we include here since it will be used in the later sections of this paper.

Following Lee (2008), we use the following tele-driving control:

$$c_1(t) := -b_1\dot{q}_1(t) - k_0 q_1(t) - k_1(q_1(t) - \overline{p_\nu}(k)) \tag{3.6}$$

$$u_\nu(t) := -b_\nu(\nu(t) - q_1(k)) \tag{3.7}$$

$$c_2(t) := -b_2\dot{q}_2(t) - k_2(q_2(t) - \overline{\phi}(k)) \tag{3.8}$$

$$u_\omega(t) := -b_\omega\dot{\phi}(t) - k_\omega(\phi(t) - \overline{q_2}(k)) \tag{3.9}$$

where (3.6)-(3.7) are the tele-accelerating control, while (3.8)-(3.9) tele-steering control; $b_\star, k_\star > 0$ are gains; and $\overline{\star}(k)$ is the modulated version of $\star(k)$ via the PSPM. We use a different definition for p_ν: instead of $p_\nu = \nu - \delta_\nu/b_\nu$ in Lee (2008), here $p_\nu := \nu + \delta_\nu/b_\nu$. We will explain this change after Th. 3.1.

Here, note that we use PSPM for c_1, c_2, u_w. Consequently we will have two-port passivity for (q_2, ϕ) mode. On the other hand, passivity/stability combination will be achieved for the (q_1, ν) mode. This is because the q_1, q_2, ϕ all are under the second-order dynamics, while ν under the first-order dynamics. As we do not use PSPM for u_ν, the PSPM for c_1 will discard excessive energy and not receive shuffled energy from the WMR side. Thus, we will use the power-shuffling scaling $\rho_s > 0$ only between c_2 and u_ω, that is, instead of (2.4), we will have: for c_2,

$$\begin{aligned} E_2(k) \Leftarrow E_2(k-1) + \Delta E_\omega(k)/\rho_s \\ + D_{2min}(k-1) - \Delta\overline{P}_2(k) \geq 0 \end{aligned} \tag{3.10}$$

while, for u_w,

$$\begin{aligned} E_\omega(k) \Leftarrow E_\omega(k-1) + \rho_s \Delta E_2(k) \\ + D_{\omega min}(k-1) - \Delta\overline{P}_\omega(k) \geq 0 \end{aligned} \tag{3.11}$$

where $\Delta E_\omega(k)/\rho_s$ and $\rho_s \Delta E_2(k)$ represent the scaled power-shuffling from the WMR and from the master, respectively.

Theorem 3.1. *Consider the master (3.5) and the dynamic WMR (3.3) under the control (3.6)-(3.9). Suppose there is no data duplication Lee and Huang (2009b). Then, the followings hold:*

1. *The closed-loop q_1-dynamics is passive, i.e. $\forall T \geq 0$, $\exists$ a bounded $c \in \Re$ s.t.*

$$\int_0^T f_1 \dot{q}_1 \geq -c^2. \tag{3.12}$$

Also, if the human operator is passive and the slave environment's instantaneous power is bounded, i.e. $\forall T \geq 0$, $\exists$ bounded constants $\alpha_1, \alpha_v \in \Re$ s.t.

$$\int_0^T f_1 \dot{q}_1 \leq \alpha_1^2, \quad \delta_v(T)\nu(T) \leq \alpha_v^2 \tag{3.13}$$

ν-dynamics is stable in the sense of bounded $\nu(t)$. On the other hand, the closed-loop (q_2, ϕ)-system is two-port passive: $\forall T \geq 0$, $\exists$ a bounded $d \in \Re$ s.t.

$$\int_0^T (\rho_s f_2 \dot{q}_2 + \delta_\omega \omega) dt \geq -d^2. \tag{3.14}$$

2. *Suppose that $E_1(k) > 0$ $\forall k \geq 1$ (i.e. enough energy for c_1 PSPM). Then, i) if $(\ddot{q}_1, \dot{q}_1, \dot{\nu}, \delta_\nu) \to 0$, $f_1 \to k_0 \nu$; or ii) if $(\ddot{q}_1, \dot{q}_1, \dot{\nu}, \nu) \to 0$, $f_1 \to -(k_0 + 2k_1)\delta_\nu / b_\nu$.*

3. *Suppose that $E_2(k) > 0$ and $E_\omega(k) > 0$ $\forall k \geq 1$ (i.e. enough energy for c_2, u_w PSPM). Then, i) if $(f_2, \delta_\omega) = 0$, $\phi \to q_2$; and ii) if $(\ddot{q}_2, \dot{q}_2, \ddot{\phi}, \dot{\phi}) \to 0$, $f_2 \to -k_2 / k_\omega \delta_\omega$.*

Proof. We have the following closed-loop dynamics with the control (3.6)-(3.9):

$$h_1 \ddot{q}_1 + b_1 \dot{q}_1 + k_0 q_1 + k_1 (q_1 - \overline{p_\nu}(k)) = f_1 \tag{3.15}$$

$$m\dot{\nu} + b_\nu (\nu - q_1(k)) = \delta_\nu \tag{3.16}$$

$$h_2 \ddot{q}_2 + b_2 \dot{q}_2 + k_2 (q_2 - \overline{\phi}(k)) = f_2 \tag{3.17}$$

$$I\ddot{\phi} + b_\omega \dot{\phi} + k_\omega (\phi - \overline{q_2}(k)) = \delta_\omega \tag{3.18}$$

For the q_1-dynamics, similar to (2.5), considering no energy shuffling for a single PSPM, we have: $\forall T \in [t_N, t_{N+1})$, s.t.

$$\int_0^T f_1 \dot{q}_1 dt \geq V_1(T) - V_1(0) + E_1(N) - E_1(0) + \sum_{i=1}^{N} \Delta E_1(i) \tag{3.19}$$

where $V_1(t) := \frac{1}{2}h_1\dot{q}_1^2 + \frac{1}{2}k_0 q_1^2 + \frac{1}{2}k_1(q_1 - \overline{p_\nu}(k))^2$. This proves the passivity of the q_1-dynamics with $c^2 = V_1(0) + E_1(0)$. The boundedness of q_1, $\dot{q}_1$ and $(q_1 - \overline{p_\nu})$ can also be shown from (3.19) with (3.13). Also, from (3.16), we have

$$\frac{d\kappa_\nu}{dt} = -b_\nu \nu^2 + b_\nu q_1(k)\nu + \delta_\nu \nu$$

where $\kappa_\nu := m\nu^2/2$. With the boundedness of $q_1(k)$ (from (3.19) with $|q_1(k)| \leq \lambda_1$) and (3.13), we have:

$$\frac{d\kappa_\nu}{dt} \leq -b_\nu |\nu|^2 + b_\nu \lambda_1 |\nu| + \alpha_\nu^2 \tag{3.20}$$

implying that $|\nu(t)|$ is ultimate bounded Khalil (1996) (i.e. $|\nu(t)| \leq \max(|\nu(0)|, (b_\nu\lambda_1 + \sqrt{b_\nu^2\lambda_1^2 + 4b_\nu\alpha_\nu^2})/(2b_\nu))$.

For the two-port passivity of (c_2, u_w), similar to (2.5), we can show that: $\forall T \geq 0$, $\exists N_1, N_2$ s.t.

$$\begin{aligned}\int_0^T f_2 \dot{q}_2 dt \geq\ & V_2(T) - V_2(0) + E_2(N_1) - E_2(0) \\ & + \sum_{i=1}^{N_1} \Delta E_2(i) - \sum_{i=1}^{N_1} \Delta E_\omega(i)/\rho_s\end{aligned}$$

$$\begin{aligned}\int_0^T \delta_\omega \omega dt \geq\ & V_\omega(T) - V_\omega(0) + E_\omega(N_2) - E_\omega(0) \\ & + \sum_{i=1}^{N_2} \Delta E_\omega(i) - \rho_s \sum_{i=1}^{N_2} \Delta E_2(i)\end{aligned}$$

where $V_2(t) := \frac{1}{2}h_2\dot{q}_2^2 + \frac{1}{2}k_2(q_2 - \overline{\phi}(k))^2$ and $V_\omega(t) := \frac{1}{2}I\dot{\phi}^2 + \frac{1}{2}k_\omega(\phi - \overline{q_2}(k))^2$. Also, with the no data duplication assumption,

$$\sum_{i=1}^{N_1}\Delta E_2(i) \geq \sum_{i=1}^{N_2}\Delta E_2(i), \quad \sum_{i=1}^{N_2}\Delta E_\omega(i) \geq \sum_{i=1}^{N_1}\Delta E_\omega(i) \tag{3.21}$$

and combining these four inequalities, we obtain

$$\begin{aligned}\rho_s \int_0^T f_2\dot{q}_2 dt + \int_0^T \delta_\omega \omega dt \\ \geq \rho_s(V_2(T) - V_2(0) + E_2(N_1) - E_2(0)) \\ + V_\omega(T) - V_\omega(0) + E_\omega(N_2) - E_\omega(0)\end{aligned}$$

which proves (3.14) with $d^2 := \rho_s V_2(0) + \rho_s E_2(0) + V_\omega(0) + E_\omega(0)$. This proves the two-port passivity with the scaling $\rho_s > 0$ of the PSPM's power-shuffling.

For the second item, when enough energy exists in the reservoir (i.e. $\overline{p_\nu} = p_\nu$), if $(\ddot{q}_1, \dot{q}_1, \dot{\nu}, \delta_\nu) \to 0$, considering $p_\nu = \nu + \delta_\nu/b_\nu \to \nu$, (3.15)-(3.16) reduce to:

$$f_1 \to k_0 q_1 + k_1(q_1 - \nu(k)), \quad 0 \to b_\nu(\nu - q_1(k)) \tag{3.22}$$

so we have $f_1 \to k_0\nu$ (the linear velocity perception). If $(\ddot{q}_1, \dot{q}_1, \dot{\nu}, \nu) \to 0$, considering $p_\nu = \nu + \delta_\nu/b_\nu \to \delta_\nu/b_\nu$, (3.15)-(3.16) reduce to:

$$f_1 \to k_0 q_1 + k_1(q_1 - \delta_\nu(k)/b_\nu), \quad \delta_\nu \to -b_\nu q_1(k) \tag{3.23}$$

so we have $f_1 \to -(k_0 + 2k_1)\delta_\nu/b_\nu$ (the force reflection).

The proof for the third item is exactly the same as that in Lee (2008), so omitted here. □

Here, a large $\rho_s > 0$ would be desirable, if the slave WMR is large or operating in a highly dissipative environment. This ρ_s may also be adapted on-line by monitoring

energy shuffling between the two systems, although its detailed exposition we spare for a future publication.

Note that p_ν provides information for operators to perceive both the WMR velocity ν and environment force δ_ν. The reason why we choose $p_\nu := \nu + \delta_\nu/b_\nu$ instead of $p_\nu = \nu - \delta_\nu/b_\nu$ Lee (2008) is that this p_ν can give an intuitive haptic perception during the transient state when WMR is affected by the environment force δ_ν. For instance, if we keep $q_1 > 0$ still (i.e. $\ddot{q}_1, \dot{q}_1$) and WMR is running steadily ($\dot{\nu} = 0$) toward the obstacle. Suppose the environment force δ_ν is rendered by some potential field method and $\delta_\nu < 0$ decreases as WMR is getting close to the obstacle, we have velocity $\nu > 0$ decreasing when WMR enters the potential field, and people can feel this resistance (i.e. increasing f_1) via the decreasing $p_\nu = \nu + \delta_\nu$. If $p_\nu = \nu - \delta_\nu$, from (3.16), we have $p_\nu = \nu - \delta_\nu/b_\nu = q_1 - m\dot{\nu}/b_\nu$. As $\dot{\nu} < 0$ decreases when WMR enters the potential field and thus p_ν increases, operator would have a confusing haptic perception ($f_1 > 0$ decreases when get close to an obstacle).

Note also that the signal p_ν for the c_1's PSPM is not purely a position signal, but rather a combination of force and velocity information. This allows us to seamlessly change haptic feedback mode between velocity feedback and force feedback as in item 2 of Th. 3.1 which corresponds the following two scenarios: cruising and hard-contact.

3.2.2 $(q_1, \nu)/(q_2, \dot{\phi})$ Tele-Driving

Instead of $q_2 \to \phi$ in Sec.3.2.1, in this tele-driving control mode, we want $q_2 \to \dot{\phi}$, which is more similar to usual car driving. Generally speaking, $q_2 \to \phi$ is suitable when we hope to keep some direction w.r.t. the global frame, and $q_2 \to \phi$ is more suitable when we want to drive freely (e.g. turning around). Noting the analogy between $q_2 \to \dot{\phi}$ problem and $q_1 \to \nu$ problem, we propose the following control

design instead of (3.8)-(3.9),

$$c_2(t) := -b_2\dot{q}_2(t) - k_0^{'}q_2(t) - k_2(q_2(t) - \overline{p_\omega}(k)) \tag{3.24}$$

$$u_\omega(t) := -b_\omega(\omega(t) - q_2(k)) \tag{3.25}$$

where $\overline{p_\omega}(k)$ is the modulated version of $p_\omega = \omega - \delta_\omega/b_\omega$ via PSPM. For tele-accelerating control, we still use (3.6)-(3.7), so the same result holds for the (q_1, ν) tele-driving mode as in 3.2.1.

Theorem 3.2. *Consider the master device (3.5) and dynamic WMR (3.3), under the tele-steering control (3.24)-(3.25).*

1. *The closed-loop q_2-dynamics is passive, similar to (3.12). If the human operator is passive and the slave environment's instantaneous power (i.e. $\delta_\omega\omega$) is bounded similar to (3.13), ω-dynamics is stable with bounded $\omega(t)$.*

2. *Suppose that $E_2(k) > 0\ \forall k \geq 1$ (i.e. enough energy for c_2 PSPM). Then, i) if $(\ddot{q}_2, \dot{q}_2, \ddot{\phi}, \delta_\omega) \to 0$, $f_2 \to k_0^{'}\omega$; or ii) if $(\ddot{q}_2, \dot{q}_2, \ddot{\phi}, \dot{\phi}) \to 0$, $f_2 \to -(k_0{}' + 2k_2)\delta_\omega/b_\omega$.*

Proof. We have the closed loop equations for the q_2-dynamics and ω-dynamics,

$$h_2\ddot{q}_2 + b_2\dot{q}_2 + k_0^{'}q_2 + k_2(q_2 - \overline{p_\omega}(k)) = f_2 \tag{3.26}$$

$$I\ddot{\phi} + b_\omega(\omega - q_2(k)) = \delta_\omega. \tag{3.27}$$

Since (3.26)-(3.27) have the same form as (3.15)-(3.16), we can similarly prove the passive q_2-dynamics and stable ω-dynamics as in Th. 3.1.

For the second item, when enough energy exists in the reservoir (i.e. $\overline{p_\omega} = p_\omega$), if $(\ddot{q}_2, \dot{q}_2, \ddot{\phi}, \delta_\omega) \to 0$, considering $p_\omega = \omega + \delta_\omega/b_\omega \to \omega$, (3.26)-(3.27) reduce to:

$$f_2 \to k_0^{'}q_2 + k_2(q_2 - \omega(k)), \quad 0 \to b_\omega(\omega - q_2(k)) \tag{3.28}$$

so we have $f_2 \to k_0'\omega$ (the angular velocity perception). If $(\ddot{q}_2, \dot{q}_2, \ddot{\phi}, \dot{\phi}) \to 0$, considering $p_\omega = \omega + \delta_\omega/b_\omega \to \delta_\omega/b_\omega$, (3.26)-(3.27) reduce to:

$$f_2 \to k_0' q_2 + k_2(q_2 - \delta_\omega(k)/b_\omega), \quad \delta\omega \to -b_\omega q_2(k) \tag{3.29}$$

so we have $f_2 \to -(k_0' + 2k_2)\delta_\omega/b_\omega$ (the torque reflection). □

Note that via p_ν and p_ω we can perceive the environment force/torque explicitly via δ_ν/δ_ω being rendered by sensors or implicitly through ν/ω changing in response of the environment (e.g. stuck by an obstacle).

3.3 Kinematic WMR Tele-Driving Control

3.3.1 $(q_1, \nu)/(q_2, \phi)$ Tele-Driving

From (3.4), since we want $q_1 \to \nu$ and $q_2 \to \phi$, we can think of the control $u_\nu = q_1(k)$, and use ν, ϕ as the set-position signals for controlling q_1 and q_2, while modulating these signals to guarantee passivity. Based on this observation, we define the control law for $(q_1, \nu)/(q_2, \phi)$ tele-driving mode, s.t.

$$c_1(t) := -b_1\dot{q}_1(t) - k_0 q_1(t) - k_1(q_1(t) - \overline{\nu}(k)) \tag{3.30}$$

$$u_\nu(t) := q_1(k) \tag{3.31}$$

$$c_2(t) := -b_2\dot{q}_2(t) - k_2(q_2(t) - \overline{\phi}(k)) \tag{3.32}$$

$$u_\omega(t) := -k_\omega(\phi(t) - \overline{q_2}(k)) \tag{3.33}$$

where $\overline{\star}(k)$ is the modulated version of $\star(k)$ via the PSPM.

We extend the original PSPM approach (which only applies to second order systems) for the first order system here. Although we do not have energy definition for kinematic systems, we can build a storage function (similar to spring energy) for the controller (3.33) as $V_\omega(t) := \frac{1}{2}k_\omega(\phi(t) - \overline{q_2}(k))^2$, and define the energy jump at t_k

by

$$\Delta\overline{P}_\omega(k) := V_\omega(t_k) - V_\omega(t_k^-). \tag{3.34}$$

Considering (3.33) and (3.4), we have: $\forall t \in [t_k, t_{k+1})$

$$\frac{dV_\omega}{dt} = k_\omega(\phi - \overline{q_2}(k))\dot{\phi} = -\dot{\phi}^2 \leq 0$$

which shows that the storage is decreasing during each interval, so we can express the loss of storage $D_\omega(k-1)$ during $[t_{k-1}, t_k)$ by,

$$D_\omega(k-1) := V_\omega(t_{k-1}) - V_\omega(t_k^-) = \int_{t_{k-1}}^{t_k} \dot{\phi}^2 dt \tag{3.35}$$

which is similar to damping dissipation. Then we can apply PSPM approach to this system with the energy jump (3.34) and the dissipation (3.35) just as we did for a second order system with spring energy jump and damping dissipation.

The following theorem summarize the main properties of this tele-driving control law (3.30)-(3.33). In contrast to the conventional tele-operation system, with the WMR being first-order kinematic, the closed-loop system is passive in the master port; while stable for the WMR port with passive human assumption.

Theorem 3.3. *Consider the master device (3.5) and the kinematic WMR (3.4), under the tele-driving control (3.30)-(3.33). Suppose that there is no data duplication. Then, the followings hold:*

1. *The closed-loop q_1-dynamics and q_2-dynamics are passive, i.e. $\forall T \geq 0$, $\exists$ bounded $d_1, d_2 \in \Re$ s.t.*

$$\int_0^T f_1\dot{q}_1 \geq -d_1^2, \quad \int_0^T f_2\dot{q}_2 \geq -d_2^2.$$

Also if the human operator is passive (3.13), ν, ω-dynamics are stable with bounded $\nu(t)$ and $\omega(t)$.

2. *Suppose that* $E_1(k) > 0\ \forall k \geq 1$ *(enough energy in* c_1 *PSPM). Then, if* $(\ddot{q}_1, \dot{q}_1) \to 0$, $f_1 = k_0\nu$.

3. *Suppose* $E_2(k) > 0$, $E_\omega(k) > 0\ \forall k \geq 1$ *(enough energy for* c_2, u_ω *PSPM). Then, if* $(f_2, \dot{\phi}) \to 0$, $q_2 \to \phi$.

Proof. We have the closed-loop q_1, q_2-dynamics s.t.

$$h_1\ddot{q}_1 + b_1\dot{q}_1 + k_0 q_1 + k_1(q_1 - \overline{\nu}(k)) = f_1 \tag{3.36}$$

$$h_2\ddot{q}_2 + b_2\dot{q}_2 + k_2(q_2 - \overline{\phi}(k)) = f_2 \tag{3.37}$$

with

$$\nu = q_1(k), \quad \dot{\phi} = -k_\omega(\phi - \overline{q_2}(k)) \tag{3.38}$$

from (3.31), (3.33). Due to the PSPMs installed both for c_1, c_2, we can get the following inequalities: $\forall T \geq 0, \exists N, N_1$ s.t.

$$\int_0^T f_1\dot{q}_1 dt \geq V_1(T) - V_1(0) + E_1(N) - E_1(0) + \sum_{i=1}^{N} \Delta E_1(i) \tag{3.39}$$

$$\begin{aligned}\int_0^T f_2\dot{q}_2 dt \geq\ & V_2(T) - V_2(0) + E_2(N_1) - E_2(0) \\ & + \sum_{i=1}^{N_1} \Delta E_2(i) - \sum_{i=1}^{N_1} \Delta E_\omega(i)/\rho_s\end{aligned} \tag{3.40}$$

where $V_1(t) := \frac{1}{2}h_1\dot{q}_1^2 + \frac{1}{2}k_0 q_1^2 + \frac{1}{2}k_1(q_1 - \overline{\nu}(k))^2$ and $V_2(t) := \frac{1}{2}h_2\dot{q}_2^2 + \frac{1}{2}k_2(q_2 - \overline{\phi}(k))^2$.

Then (3.39) suggests passive q_1-dynamics with $d_1^2 = V_1(0) + E_1(0)$, and also implies bounded ν with (3.13). For the controller u_ω installed with PSPM, considering (2.6) and the definitions for $\Delta\overline{P}_\omega(k)$ (3.34) and $D_\omega(k-1)$ (3.35), we have: $\forall T \geq 0, \exists N_2$

s.t.

$$
\begin{aligned}
&V_\omega(T) - V_\omega(0) \\
&\quad = [V_\omega(T) - \sum_{i=1}^{N_2} \Delta\overline{P}_\omega(i) - V_\omega(0)] + \sum_{i=1}^{N_2} \Delta\overline{P}_\omega(i) \\
&\quad = [V_\omega(T) - V_\omega(t_{N_2}) - \sum_{i=0}^{N_2-1} D_\omega(i)] + \sum_{i=1}^{N_2} \Delta\overline{P}_\omega(i) \\
&\quad \leq -\int_{t_{N_2}}^{T} \dot{\phi}^2 dt - \sum_{i=1}^{N_2} [D_{\omega min}(i-1) - \Delta\overline{P}_\omega(i)] \\
&\quad \leq -\sum_{i=1}^{N_2} [E_\omega(i) - E_\omega(i-1) + \Delta E_\omega(i) - \rho_s \Delta E_2(i)] \\
&\quad = -E_\omega(N_2) + E_\omega(0) - \sum_{i=1}^{N_2} \Delta E_\omega(i) + \rho_s \sum_{i=1}^{N_2} \Delta E_2(i)
\end{aligned} \tag{3.41}
$$

which can be rearranged to

$$
\begin{aligned}
0 \geq\ & V_\omega(T) - V_\omega(0) + E_\omega(N_2) - E_\omega(0) \\
& + \sum_{i=1}^{N_2} \Delta E_\omega(i) - \rho_s \sum_{i=1}^{N_2} \Delta E_2(i).
\end{aligned} \tag{3.42}
$$

With the no data duplication assumption, adding (3.40) and (3.42), we have:

$$
\begin{aligned}
\rho_s \int_0^T f_2 \dot{q}_2 dt \geq\ & \rho_s (V_2(T) - V_2(0) + E_2(N_1) - E_2(0)) \\
& + V_\omega(T) - V_\omega(0) + E_\omega(N_2) - E_\omega(0)
\end{aligned}
$$

which proves the passive q_2-dynamics with $d_2^2 = \rho_s V_2(0) + \rho_s E_2(0) + V_\omega(0) + E_\omega(0)$; and also proves bounded $V_\omega(t)$, bounded $\phi - \overline{q_2}(k)$ and bounded $\omega(t)$, with the passive human assumption.

For the second item, if there is enough energy in the reservoir E_1, $\overline{\nu}(k) = \nu(k)$. From (3.4) and (3.31), we have $\nu = u_\nu = q_1(k)$. Then if $(\ddot{q}_1, \dot{q}_1) \to 0$, equation (3.36) gives $f_1 \to k_0 \nu$. For the third item, when enough energy exists in the reservoirs,

$\overline{\phi}(k) = \phi(k)$ and $\overline{q_2}(k) = q_2(k)$, if $\dot{\phi} \to 0$, we have $\phi(k+1) \to \phi(k)$. Following the result in (Lee and Huang, 2009b, Th. 1), we have $q_2 \to \phi$. □

For this mode we can choose ρ_s to be small, since one could assume that the environment force is zero for a kinematic WMR and that there is no energy disspation to the environment.

3.3.2 $(q_1, \nu)/(q_2, \dot{\phi})$ Tele-Driving

The $(q_2, \dot{\phi})$ tele-driving mode is similar to (q_1, ν) tele-driving mode in 3.3.1, so we can use (3.30)-(3.31) for tele-accelerating control and the following control for the $(q_2, \dot{\phi})$ tele-driving mode:

$$c_2(t) := -b_2\dot{q}_2(t) - k_0^{'}q_2(t) - k_2(q_2(t) - \overline{\omega}(k)) \tag{3.43}$$

$$u_\omega(t) := q_2(k) \tag{3.44}$$

The following theorem can be proved similarly to Th. 3.3, so we omit its proof here.

Theorem 3.4. *Consider the master device (3.5) and the kinematic WMR (3.4), under the tele-steering control (3.43)-(3.44).*

1. *The closed-loop q_2-dynamics is passive, and the ω-dynamics is stable with bounded $\omega(t)$ under the passive human assumption (3.13).*

2. *Suppose $E_2(k) > 0\ \forall k \geq 1$ (enough energy in c_2 PSPM), if $(\ddot{q}_2, \dot{q}_2) \to 0$, we have $f_2 = k_0^{'}\omega$.*

Chapter 4

Quad-rotor type UAV tele-operation over the Internet

4.1 Problem Setting of UAV teleoperation

We consider a quadrotor type UAV evolving on $SE(3)$ with the following translational dynamics and attitude kinematics Hua et al. (2009):

$$m\ddot{x} = -\lambda R e_3 + mge_3 + \delta \tag{4.1}$$

$$\dot{R} = RS(\omega) \tag{4.2}$$

where $m > 0$ is the mass, $x \in \Re^3$ is the Cartesian position w.r.t. the NED (north-east-down) inertial frame with e_3 representing its down-direction, $\lambda \in \Re$ is the thrust along the body-frame down direction, $\delta \in \Re$ is the Cartesian disturbance, $R \in SO(3)$ is the rotational matrix describing the body NED frame of UAV w.r.t. the inertial NED frame, $\omega := [\omega_1, \omega_2, \omega_3] \in \Re^3$ is the angular velocities of the body frame relative to the inertial frame expressed in the body frame, $J \in \Re^{3\times3}$ is the inertia matrix w.r.t. the body frame, g is the gravitational constant, and $S(\star) : \Re^3 \to so(3)$ is the skew-symmetric operator defined s.t. for $a, b \in \Re^3, S(a)b = a \times b$.

The control input for this quadrotor-type UAV are $\lambda \in \Re$ and the angular rate $\omega \in \Re^3$. Since the available control for the UAV is only 4-dimensional while its evolution is in 6-dimensional space ($SE(3) = E^3 \times SO(3)$), this implies the UAV is not fully actuated. More specifically, its Cartesian motion (4.1) can be affected by the thrust λ, although its direction is coupled to the attitude kinematics (4.2). Usually, if we control the UAV through a transmitter, lots of training is needed before operator can smoothly control the UAV, and trying to maintain its attitude would distract the operator from the main tasks like surveillance or transportation. For this, we design a back-stepping trajectory tracking controller so that the operator only need to care about the Cartesian position of the UAV while the UAV automatically control the attitude and follow the desired Cartesian position.

4.2 Backstepping trajectory tracking control of UAVs

4.2.1 Controller Design

By inspecting the translational dynamics (4.1), we first define the following desired control ν:

$$\nu := -m\ddot{x}_d + mge_3 + b\dot{e} + ke \tag{4.3}$$

where $x_d(t) \in \Re^3$ is the desired trajectory, $e(t) := x(t) - x_d(t)$ is the tracking error, and $b, k > 0$ are damping/spring gains. Our wish is to let the term λRe_3 in (4.1) to be the same as the virtual control ν yet we can not directly control the rotation matrix R, that is, there would be some error betweeen them and define the control generation error ν_e s.t.

$$\nu_e = \lambda Re_3 - \nu \tag{4.4}$$

Here, to derive our "nominal" control, we assume no Cartesian disturbance with $\delta = 0$ in (4.1). we will analyze its effect in Sec. 4.2.2.

By (4.1), (4.3) and (4.4), we can write the closed-loop dynamics:

$$m\ddot{e} + b\dot{e} + ke = \nu_e \tag{4.5}$$

for which we define the first Lyapunov function

$$V_1 := \frac{1}{2}m\dot{e}^T\dot{e} + m\epsilon e^T\dot{e} + \frac{1}{2}(k + \epsilon b)e^T e \tag{4.6}$$

where $\epsilon > 0$ is a constant to be chosen below. The term with ϵ is called cross-coupling term to achieve exponential convergence for the above linear second-order dynamics with $\nu_e = 0$ (**?**). Differentiate V_1 with (4.5), we then have

$$\dot{V}_1 = -(b - m\epsilon)\dot{e}^T\dot{e} - \epsilon k e^T e - (\dot{e} + \epsilon e)^T\nu_3 \tag{4.7}$$

Here we define the following two matrix P, Q and vector ζ s.t.

$$P := \begin{bmatrix} m & \epsilon m \\ \epsilon m & k + \epsilon b \end{bmatrix} \otimes I_3, \qquad Q := \begin{bmatrix} b - \epsilon m & 0 \\ 0 & \epsilon k \end{bmatrix} \otimes I_3, \qquad \zeta := \begin{bmatrix} \dot{e} \\ e \end{bmatrix} \tag{4.8}$$

with $P, Q \succ 0$ if $0 < \epsilon < b/m$, then we have

$$V_1 = \zeta^T P \zeta, \qquad \dot{V}_1 = -\zeta^T Q \zeta - (\dot{e} + \epsilon e)^T\nu_e \tag{4.9}$$

From (4.9), if $\nu_e = 0$, we would have $(\dot{e}, e) \to 0$ exponentially. Aiming to bound ν_e about the origin we augment V_1 s.t.

$$V_2 = V_1 + \frac{1}{2\gamma}\nu_e^T\nu_e \tag{4.10}$$

where $\gamma > 0$ is a constant, which would be helpful for the robustness analysis in Sec. 4.2.2. Differentiating V_2 we have

$$\dot{V}_2 = -\frac{b}{2}\dot{e}^T\dot{e} - \epsilon k e^T e + \frac{1}{\lambda}\nu_e^T(\dot{\nu}_e - \gamma(\dot{e} + \epsilon e)) \tag{4.11}$$

If we use the following update law for $\dot{\nu}_e$ s.t.

$$\dot{\nu}_e = \gamma(\dot{e} + \epsilon e) - \alpha\nu_e \tag{4.12}$$

we can have

$$\dot{V}_2 = -\frac{b}{2}\dot{e}^T\dot{e} - \epsilon k e^T e - \frac{\alpha}{\gamma}\nu_e^T\nu_e \tag{4.13}$$

implying exponential convergence of $e, \dot{e}$ and ν_e.

The control design for (λ, ω) is in fact From (4.2) and (4.12), we have

$$\dot{\nu}_e + \alpha\nu_e = R\dot{\lambda}e_3 + \dot{R}\lambda e_3 - \dot{\nu} + \alpha(\lambda R e_3 - \nu) = R\begin{pmatrix} \lambda\omega_2 \\ -\lambda\omega_1 \\ \dot{\lambda} + \alpha\lambda \end{pmatrix} - \dot{\nu} - \alpha\nu \tag{4.14}$$

, from which and (4.12), we have the following control law in the following form:

$$R\begin{pmatrix} \lambda\omega_2 \\ -\lambda\omega_1 \\ \dot{\lambda} + \alpha\lambda \end{pmatrix} = \dot{\nu} + \alpha\nu + \gamma(\dot{e} + \epsilon e) := \bar{\nu} \quad \text{or} \quad \begin{pmatrix} \lambda\omega_2 \\ -\lambda\omega_1 \\ \dot{\lambda} + \alpha\lambda \end{pmatrix} = R^T\bar{\nu} \tag{4.15}$$

where $\dot{\nu}$ in $\bar{\nu}$ can be computed by

$$\dot{\nu} = -m\dddot{x}_d - b\ddot{x}_d + k\dot{e} + \frac{b}{m}(-\lambda R e_3 + mge_3) \tag{4.16}$$

From equation (4.15) we can get the control law for $(\lambda, \omega_1, \omega_2)$ as long as $\lambda \neq 0$. The singularity at $\lambda = 0$ seems not likely happen in practice unless operator command the UAV to "free-fall" (Frazzoli et al. (2000)).

The relation(4.15) also shows that any (smooth) desired control ν can be incorporated into our backstepping control design, as long as it produce a relation similar to (4.15) and its computation is implementable similar to $\dot{\nu}$ in (4.16) hear. Also, note that the control parameters b, k, α have clear physical meanings, thereby, making the tuning very intuitive. These manifest the flexibility and transparency of our backstepping control law. Note also from (4.15) that, in order to produce the desired control ν, we only need $\lambda, \omega_1, \omega_2$, not ω_3. In other words, this ω_3 is redundant, and we may simply set $\omega_3 = 0$ or use it for other purpose (e.g. to head to a certain direction while flying). This also reaffirms the well-known fact (e.g. Aguiar and Hespanha (2007)) that, for a thrust-propelled rigid body on $SE(3)$, we only need one thrust force and two angular rates along the other two (body) axes to control its Cartesian motion in E^3. The following Th. 4.1 summarizes our backstepping trajectory tracking control design and its key properties.

Theorem 4.1. *Consider the UAV (4.1)-(4.2) under the backstepping control (4.15) with ω_3 and $\dot{x}_d, \ddot{x}_d, \dddot{x}_d$ being all bounded. Suppose that $\exists \epsilon_\lambda > 0, s.t. \lambda(t) \geq \epsilon_\lambda \forall t \geq 0$. Then $(\dot{e}, e, \nu_e) \to 0$ exponentially; and $(\ddot{x}, \dot{x}, \lambda, \omega)$ are bounded.*

Proof. Exponential convergence of $(\dot{e}, e, \nu_e)$ and their boundedness have already been shown above. λ is bounded from (4.4) with bounded ν_e and ν. $\dot{\nu}$ is bounded from (4.16), which implies $\bar{\nu}$ is also bounded with its definition in (4.15). Thus, from (4.15) with the assumption that $\lambda(t) \geq \epsilon_\lambda > 0$, ω_1, ω_2 are bounded. Also the boundedness of ω_3 and $\ddot{x}$ can be easily seen from $\omega_3 = 0$ and (4.5). □

4.2.2 Robustness Analysis

In this section we will analyze the robustness of the backstepping control in the presence of unknown/bounded disturbance δ and inaccurate estimate of m (identified w.r.t. a certain unit of λ).

Here, the desired control ν is given by

$$\nu = -\hat{m}\ddot{x}_d + \hat{m}ge_3 + b\dot{e} + ke \tag{4.17}$$

where $\hat{m} := m + \tilde{m} > 0$ is the estimate of the UAV mass m; and, instead of (4.5), the closed-loop dynamics is given by

$$m\ddot{e} + b\dot{e} + ke = -\nu_e - d \tag{4.18}$$

where $d := -\tilde{m}\ddot{x}_d + \tilde{m}ge_3 - \delta$ is the combined (bounded) effect of the uncertain m and the disturbance δ. Using the same V_1 as in (4.9), we have

$$\dot{V}_1 = -\frac{b}{2}\dot{e}^T\dot{e} - \epsilon k e^T e - (\dot{e} + \epsilon e)^T(\nu_e + d) \tag{4.19}$$

and, using the same V_2 as in (4.10), we have

$$\dot{V}_2 = -\frac{b}{2}\dot{e}^T\dot{e} - \epsilon k e^T e + \frac{1}{\gamma}\nu_e^T(\dot{\nu}_e - \gamma(\dot{e} + \epsilon e)) - (\dot{e} + \epsilon e)^T d \tag{4.20}$$

where the last term cannot distabilize the system, since d is bounded.

The above inequality suggests that we can use the same update law (4.12) for ν_e. This (4.12) may not appear to require the correct estimate of m. Yet, if we inspect its decoding (4.15) and (4.16), which gives the actual control action (λ, ω); we will find that this update law (4.12) will require us to have a information of $\ddot{x}$, which is estimated by $\ddot{x} = \frac{1}{\hat{m}}(-\lambda Re_3 + \hat{m}ge_3)$. Here note that, even with uncertain m, $\nu_e = \lambda Re_3 - \nu$ in (4.4) is still certain, since λRe_3 and ν are known (although not necessarily accurate). If we use the possible incorrect estimate $\hat{m}$ for $\ddot{x}$, which then comes into $\dot{\nu}$ (4.16) and $\bar{\nu}$ (4.15), we end up with

$$\dot{\nu}_e = \gamma(\dot{e} + \epsilon e) - \alpha\nu_e + e_{m^{-1}}b\lambda Re_3 - \frac{b}{m}\delta \tag{4.21}$$

where $e_{m^{-1}} := (1/m - 1/\hat{m}) = \tilde{m}/(m\hat{m})$ is due to the uncertainty in m.

Inserting this (imperfect) update law into the above $\dot{V}_2$ and using the definition of ν_e (4.4) and ν (4.17), we have:

$$\begin{aligned}
\dot{V}_2 &= -\frac{b}{2}\dot{e}^T e - \epsilon k e^T e - \frac{\alpha}{\gamma}\nu_e^T \nu_e + \frac{b e_{m^{-1}}}{\gamma}\nu_e^T(\nu_e + \nu) - \frac{b}{\gamma m}\nu_e^T \delta - (\dot{e} + \epsilon e)^T d \\
&= -\frac{b}{2}\dot{e}^T e - \epsilon k e^T e - \frac{\alpha}{\gamma}\nu_e^T \nu_e - (-\frac{b^2 e_{m^{-1}}}{\gamma})\nu_e^T \dot{e} - (-\frac{bke_{m^{-1}}}{\gamma})\nu_e^T e \\
&\quad - \frac{b e_{m^{-1}}}{\gamma}\nu_e^T(\hat{m}\ddot{x}_d - \hat{m}ge_3) - \frac{b}{\gamma m}\nu_e^T \delta - (\dot{e} + \epsilon e)^T d \\
&= -\bar{\zeta}^T Q' \bar{\zeta} - \frac{b e_{m^{-1}}}{\gamma}\nu_e^T \hat{d} - (\dot{e} + \epsilon e)^T d
\end{aligned} \tag{4.22}$$

where $\bar{\zeta} := [\dot{e}; e; \nu_e]$, $\hat{d} = -\hat{m}\ddot{x}_d + \hat{m}ge_3 + \frac{\delta}{me_{m^{-1}}}$, and Q' is defined as

$$Q' := \begin{bmatrix} \frac{b}{2} & 0 & -\frac{b^2 e_{m^{-1}}}{2\gamma} \\ 0 & \epsilon k & -\frac{bke_{m^{-1}}}{2\gamma} \\ -\frac{b^2 e_{m^{-1}}}{2\gamma} & -\frac{bke_{m^{-1}}}{2\gamma} & \frac{\alpha - be_{m^{-1}}}{\gamma} \end{bmatrix}$$

Then, following Horn and Johnson (2005), we can set $Q' \succ 0$ by choosing α, γ, b, k s.t.

$$\alpha \geq be_{m^{-1}} + \frac{b^2 e_{m^{-1}}^2 (2\epsilon b + k)}{4\epsilon\gamma}. \tag{4.23}$$

This implies even with the uncertain m and unknown/bounded δ, the system will still be stable with $(\dot{e}, e, \nu_e)$ being ultimately bounded Khalil (1996).

Note that, given the estimation error $e_{m^{-1}}$ and b, k, this condition (4.23) is always grantable, if we choose α and γ large enough. Large α, γ are possible as they only affect the system behavior in software. On the other hand, the ultimate bound of $(\dot{e}, e, \nu_e)$ is likely shrinking with large b, k. Yet b, k are not freely tunable because large b, k may cause the system to reach the limitation of hardware (i.e. actuator saturation). It is also worthwhile to mention that, in many cases, it is not so difficult to estimate m fairly precisely (e.g. less than 5% error for our experiment in Chapter

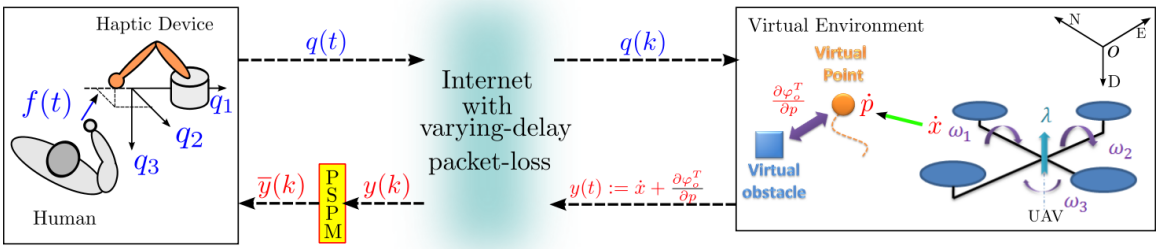

Figure 4.1: UAV teleoperation. The velocity of the virtual point $\dot{p}$ is controlled by the configuration of the hapitc device q, and affected by the repulsion $\frac{\partial \varphi_o^T}{\partial p}$ from the virtual obstacle. The UAV follows the virtual point through a backstepping controller

5). Note also that we can also try to cancel out the disturbance δ by putting an estimate $\hat{\delta}$ in ν (4.17) to enhance the control performance.

4.3 Application to UAV teleoperation over the Internet

4.3.1 Virtual Point and Virtual Environment

In this section, we show how the backstepping control can be used for the UAV haptic teleoperation over th Internet. We consider a virtual point (VP) evolving according to

$$\dot{p} = \eta q(k) - \frac{\partial \varphi_0^T}{\partial p} \tag{4.24}$$

where $p \in \Re^3$ is the VP's position, $q(k) \in \Re^3$ is the master position received via the Internet at time t_k, $\eta > 0$ is to match different scales between $q(t)$ and $\dot{p}$, and $\varphi_o(||p - p_o||)$ is the obstacle avoidance potential, producing repulsive force when $||p - p_o||$ becomes small.

The control $\eta q(k)$ enables the user to tele-control the VP's velocity $\dot{p}$ by the master device's position $q(t)$, thereby, to circumvent the problem of master-slave kinematic dissimilarity (i.e. stationary master with bounded workspace; mobile VP

with unbounded workspace Lee et al. (2006a)). The kinematic VP is also chosen here in contrast to the second-order/dynamic VPs (**?**), since it greatly simplifies the stability and collision avoidance analysis as shown below.

Since we also need to compute $\dot{p}, \ddot{p}, \dddot{p}$ for UAV trajectory tracking control, and time derivative for $p(k)$ is not well-defined, we remedy this by changing (4.24) to the following:

$$\dot{p} = \eta\bar{q}(t) - \frac{\partial\varphi_o^T}{\partial p} \tag{4.25}$$

where $\bar{q}(t)$ is defined s.t.

$$\ddot{\bar{q}}(t) + b^{'}\dot{\bar{q}} + k^{'}\bar{q}(t) = a^2 q(k) \tag{4.26}$$

i.e. second-order critically damped filter with $a > 0, b^{'} = 2a, k^{'} = a^2$. Here, note that, due to the second-order nature, $\ddot{\bar{q}}(t), \dot{\bar{q}}(t), \bar{q}(t)$ are all bounded as long as $q(k)$ is bounded, regardless of discontinuity of $q(k)$. If we set a to be large enough, we can practically ensure $||q(k) - \bar{q}(k)||$ to be small enough. Since the VP (4.25) dynamics is simulated in software, we may indeed choose this a to be large enough if that is desired. Now we can compute $\ddot{p}, \dddot{p}$ as follows:

$$\ddot{p} = -H_{\varphi_o}(p)\dot{p} + \eta\dot{\bar{q}}(t) \tag{4.27}$$

$$\begin{aligned}\dddot{p} &= -\frac{dH_{\varphi_o}(p)}{dt}\dot{p} - H_{\varphi_o}\ddot{p} + \eta\ddot{\bar{q}}(t) \\ &= -\frac{dH_{\varphi_o}(p)}{dt}\dot{p} + H_{\varphi_o}(p)[H_{\varphi_o}(p)\dot{p} - \eta\dot{\bar{q}}(t)] - \eta[b^{'}\dot{\bar{q}}(t) + k^{'}(\bar{q}(t) - q(k))]\end{aligned} \tag{4.28}$$

where $H_{\varphi_o}(p) := [\frac{\partial^2\varphi_o}{\partial p_i \partial p_j}] \in \Re^3$ is the Hessian of φ_o.

Let us define a Lyapunov function to analyze the stability of the $p-$dynamics and $\bar{q}-$dynamics s.t.

$$V_p := \varphi_o + \frac{1}{2}||\dot{\bar{q}}||^2 + \bar{\epsilon}\dot{\bar{q}}^T\bar{q} + \frac{1}{2}(k^{'} + \bar{\epsilon}b^{'})||\bar{q}||^2 = \varphi_o + [\dot{\bar{q}}; \bar{q}]^T Q[\dot{\bar{q}}; \bar{q}] \tag{4.29}$$

where $\bar{\epsilon} > 0$ is choose by (4.31) and Q is defined as

$$Q = \begin{bmatrix} \frac{1}{2} & \frac{1}{2}\bar{\epsilon} \\ \frac{1}{2}\bar{\epsilon} & \frac{1}{2}(k^{'} + \bar{\epsilon}b^{'}) \end{bmatrix}$$

From (4.25) and (4.26), we have

$$\frac{dV_p}{dt} = -\zeta^T \bar{Q}\zeta - u^T\zeta \leq -\underline{\sigma}[\bar{Q}] \cdot ||\zeta||^2 + ||u|| \cdot ||\zeta|| \tag{4.30}$$

where $\zeta := [\partial\varphi_o^T \partial p; \bar{q}; \dot{\bar{q}}]$, and $u := k^{'} q(k) \cdot [0; \bar{\epsilon}; 1] \otimes I_3$ and $\underline{\sigma}[\bar{Q}]$ is the minimum singular value of $\bar{Q}$ with

$$\bar{Q} := \begin{bmatrix} 1 & -\frac{\eta}{2} & 0 \\ -\frac{\eta}{2} & \bar{\epsilon}k^{'} & 0 \\ 0 & 0 & b^{'} - \bar{\epsilon} \end{bmatrix}.$$

Here we want $Q, \bar{Q} \succ 0$, thus, we can choose ϵ as follows

$$\bar{\epsilon}^2 - b^{'}\bar{\epsilon} - k^{'} < 0, \quad \bar{\epsilon} < b, \quad \bar{\epsilon}k^{'} > \eta^2/4$$

which can be simplified as:

$$\eta^2/(4k^{'}) < \bar{\epsilon} < b^{'} \tag{4.31}$$

The inequality (4.30) also implies that, similar to the case of ultimate boundedness, if $||\zeta|| \geq \frac{||u||}{\underline{\sigma}[Q]}$, we will have $\dot{V}_p \leq 0$.

Based on this observation, we have the following Prop. (1), for which we assume that φ_o is constructed s.t. 1) there exists a large enough $\bar{M} > 0$ s.t. $V(t) \leq \bar{M}$ implies no collision with the obstacle, and 2) $||\partial\varphi_o/\partial p||$ is bounded if $\varphi_o(||p - p_o||)$ is bounded.

Proposition 1. *Suppose $q(k)$ is bounded $\forall k \geq 0$. Suppose further that, if $\varphi_o(||p - p_o||) \geq \bar{M}$,*

$$||\frac{\partial\varphi_o}{\partial p}|| \geq \frac{k^{'} q_{max}\sqrt{1 + \bar{\epsilon}^2}}{\underline{\sigma}[\bar{Q}]} \tag{4.32}$$

Then, $\varphi_o \leq \bar{M} \forall t \geq 0$ *and* $\bar{q}, \dot{\bar{q}}, \ddot{\bar{q}}$ *are bounded. Suppose further that* $H_{\varphi_o}, \frac{dH_{\varphi_o}}{dt}$ *are bounded if* $\varphi_o \leq \bar{M}$*. Then* $\dot{p}, \ddot{p}, \dddot{p}$ *are all bounded.*

Proof. The inequality implies that, if $||\zeta|| \geq \frac{||u||}{\underline{\sigma}[Q]}, \dot{V}_p \leq 0$. With the above condition (4.32), if $\varphi_o \geq \bar{M}$, we have

$$||\zeta|| \geq ||\frac{\partial \varphi_o}{\partial p}|| \geq \frac{||u||}{\underline{\sigma}[\bar{Q}]} \tag{4.33}$$

which further implies that

$$\varphi_o \leq V_p(t) \leq \bar{M}$$

and that $\frac{\partial \varphi_o}{\partial p}, H_{\varphi_o}, \frac{dH_{\varphi_o}}{dt}$ are bounded. The boundedness of $\bar{q}, \dot{\bar{q}}, \ddot{\bar{q}}$ is a direct consequence of the mass-spring-damper type dynamics (4.26), and the boundedness of $\dot{p}, \ddot{p}, \dddot{p}$ can be deduced from equation (4.25), (4.27) and (4.28). □

Now given that $\dot{p}, \ddot{p}, \dddot{p}$ are all well-defined, the backstepping control can the robustly enable the UAV to track the trajectory of the VP. Here, we assume the obstacle is designed s.t. it rapidly increases as the VP approaches the obstacle to prevent collision; while gradually converge to zero as $||p - p_o|| \to 0$ so that the effect of the obstacle can smoothly emerges when they gets close to the VP.

One possible potential function, if we define $||x|| := ||p - p_o||$ could be

$$\varphi_o(||x||) := \begin{cases} k(\frac{||x||^2 - d^2}{||x||^2 - \mu^2})^2 & \mu < ||x|| \leq d \\ 0 & ||x|| > d \end{cases}$$

with

$$\frac{\partial \varphi_o}{\partial p} = 4k(d^2 - \mu^2)\frac{||x||^2 - d^2}{(||x||^2 - \mu^2)^3}(p - p_o)^T$$

where $d > \mu > 0$. Other form of potential field (e.g. Ji and Egerstedt (2005)) is also possible.

4.3.2 Control Design for Haptic Device

For the haptic device control design, we use passive set-position modulation framework again to address the kinematic/dynamic discrepancy between the master device (fully-actuated Lagrangian dynamics with bounded workspace) and the VPs (kinematic system with unbounded workspace), and to guarantee passivity/stability over the Internet with useful haptic feedback.

We consider 3-DOF haptic device with the following dynamics:

$$M(q)\ddot{q} + C(q,\dot{q})\dot{q} = \tau + f \tag{4.34}$$

where $q \in \Re^3$ is the configuration, $M(q) \in \Re^{3\times3}$ is the positive-definite/symmetric inertia matrix, $C(q,\dot{q}) \in \Re^{3\times3}$ is the Coriolis matrix, and $\tau, f \in \Re^3$ are the control and human forces, respectively. For the control of the haptic device, we first design a feedback signal $y(t) \in \Re^3$ received on the master side, s.t.

$$y(t) := \frac{1}{\eta}(\dot{x} - \frac{\partial \phi_o^T}{\partial p}) \tag{4.35}$$

where $\dot{x}$ is the UAV's velocity in (4.1) and $-\frac{\partial \phi_o^T}{\partial p}$ is the virtual environment force. This feedback allows operator to perceive the state of the real UAV and to sense the presence of the obstacle on VP.

This $y(t)$ is then sent back to the master side over the Internet. Let $y(k)$ denote the signal received on the master side, then, similar to the control design in Chapter 3, we can design the control τ s.t. for $t \in [t_k, t_{k+1})$,

$$\tau(t) := -B\dot{q} - K_1 q - K(q - \bar{y}(k)) \tag{4.36}$$

where $B, K_1, K \succ 0$ are diagonal gain matrices, and $\bar{y}(k)$ is the PSPM modulated version of $y(k)$, s.t.

$$\min_{\bar{y}k} ||y(k) - \bar{y}(k)|| \tag{4.37}$$

$$subj. E(k) = E(k-1) + D_{min}(k-1) - \Delta\bar{P}(k) \geq 0 \tag{4.38}$$

Note in this case, only one PSPM is used on the master side, the excessive energy in the PSPM would be discarded. Now we can summarize the result in this chapter.

Theorem 4.2. *Consider the master device (4.34) with control (4.36). Then the follows hold:*

1. *The closed-loop master system is passive:* $\exists c_1 \in \Re$ *s.t.* $\int_0^T f^T \dot{q} \geq -c_1^2, \forall T \geq 0$. *Moreover, if the human user is also passive (i.e.* $\exists c_2 \in \Re$, *s.t.* $\int_0^T f^T \dot{q} dt \leq c_2^2, \forall T \geq 0$*), the closed-loop VPs teleoperation system is stable, with* $q, \dot{q}, q - \bar{y}(k)$ *and* p *being all bounded.*

2. *Suppose* $\ddot{q}, \dot{q} \to 0, E(k) \geq 0 \forall k \geq 0$, *and* $\dot{x} \to \dot{p}$. *Then, a) if* $-\frac{\partial \varphi_0^T}{\partial p} = 0$ *(e.g. no obstacles),* $f(t) = \frac{K_1}{\eta}\dot{x}$ *(i.e. velocity perception); or b) if* $\dot{x} = 0$ *(e.g. stopped by obstacles),* $f(t) \to \frac{K_1 + 2K}{\eta}\frac{\partial \varphi_o^T}{\partial p}$ *(i.e. environment force perception)*

Proof. For the first item, following the same procedure as in Lee and Huang (2009b), we can show that $\forall T \geq 0$,

$$\int_0^T f^T \dot{x} dt \geq V_m(T) - V_m(0) + E(N_T) - E(0) \tag{4.39}$$

where $V_m(t) := ||\dot{q}||_M^2/2 + ||q(t_k) - \bar{y}(k)||_K^2/2 + ||q||_{K_1}^2$, and N_T is the k-index happening just before T. From (4.39), we can show the master passivity with $c_1^2 = V_m(0) + E(0)$ and bounded $q, \dot{q}, q - \bar{y}(k)$ and p with the passive human assumption.

For the second item, if $\ddot{q}, \dot{q} \to 0$ and $E(k) \geq 0 \forall k \geq 0$ (i.e. $\bar{y}(k) = y(k)$), the closed-loop master dynamic becomes

$$K_1 q + K(q - y(k)) \to f(t) \tag{4.40}$$

with $q(t) \to q$ and $-\frac{\partial \varphi_0^T}{\partial p} = 0$, we have $\dot{p} \to \eta \bar{q} \to \eta q(k) \to \eta q$. Thus if $\dot{x} \to \dot{p}$, we have $f(t) = \frac{K_1}{\eta} \dot{x}$. If $\dot{x} = 0$, thus $p \to 0$ from the assumption, and from (4.25) we have

$$0 = q - \frac{\partial \varphi_0^T}{\partial p}, \quad y = -\frac{1}{\eta} \frac{\partial \varphi_0^T}{\partial p}$$

, then, with (4.40), we have $f(t) \to \frac{K_1 + 2K}{\eta} \frac{\partial \varphi_o^T}{\partial p}$. □

Chapter 5

Experiment

5.1 WMR haptic tele-driving Experiment

We use a Phantom Desktop as the master device, and a differential wheeled mobile robot as the slave WMR, see Fig 3.1. we use three ultrasonic rangefinders fixed at the front of the WMR to render external repulsion (e.g. δ_ν or δ_ω) from obstacles. This virtual force/torque will exert on the robot and also be perceived by human (through $p_\nu = \nu + \delta_\nu/b_\nu$ or $p_\omega = \omega + \delta_\omega/b_\omega$). The local servo-rates for the haptic device and WMR are 1ms and 2ms respectively. They are connected over WLAN (wireless local area network) with data buffering to set the communication delay. Two magnitudes of round-trip delay are considered: randomly ranging from 0.25sec to 0.35sec (0.125∼0.175sec forth plus 0.125∼0.175sec back) corresponding to intercontinental tele-operation over Internet Elhajj et al. (2001)), and another ranging from 1sec to 2sec (0.5∼1sec forth plus 0.5∼1sec back). The packet-loss is around 90% and packet-to-packet separation time is 15∼300ms with an average of about 50ms.

We use linear/angular motion scaling η_1/η_2 and energy scaling ρ to scale the haptic device side to match the mechanical scale of the WMR. Energy shuffling scaling ρ_s is also used to enlarge/shrink energy shuffled between haptic device and WMR, if PSPM is used on both sides.

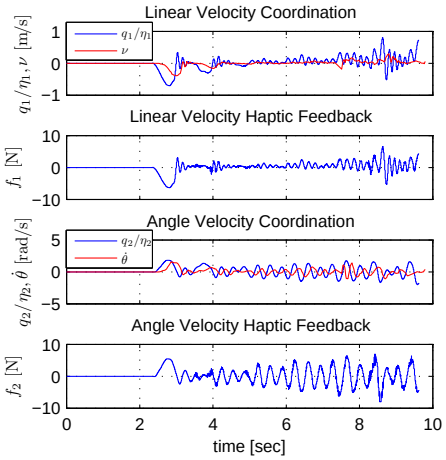

Figure 5.1: Unstable case: dynamic WMR $(q_1, \nu)/(q_2, \dot{\phi})$ tele-driving with 0.25∼0.35sec randomly varying delay without using PSPM

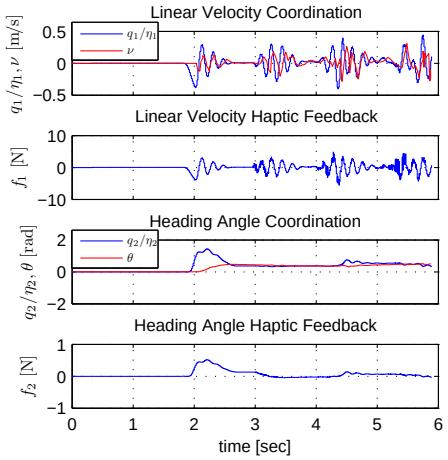

Figure 5.2: Unstable case: kinematic WMR $(q_1, \nu)/(q_2, \phi)$ tele-driving with 0.25∼0.35sec randomly varying delay without using PSPM

Experiments are shown for tele-driving with 0.25∼0.35sec randomly varying delay in dynamic WMR $(q_1, \nu)/(q_2, \dot{\phi})$ mode and kinematic WMR $(q_1, \nu)/(q_2, \phi)$ mode without using PSPM, as shown in Fig. 5.1 / Fig. 5.2. We pull the haptic device with a moderate force at 2.5sec / 2sec and release it, then the systems become unstable. Then we make the same experiments when PSPM is utilized. As shown in Fig. 5.3 / Fig. 5.4, after the disturbance given from the master side, the systems are stabilized and (q_1, ν), $(q_2, \phi/\dot{\phi})$ are coordinated. Note the received signals are modified by PSPM to avoid the accumulation of energy jump whenever the energy in the reservoir depletes. Also by inspecting the changing of energy reservoirs in Fig. 5.4, we can see the (q_1, ν) control is more likely to be destabilized than (q_2, ϕ) control, with certain controller parameters as in our case. Also, we can see from Fig. 5.2 and Fig. 5.4 that q_2 does not return to zero. This is due to the friction for the q_2-DOF on the master side.

Now we test the dynamic WMR $(q_1, \nu)/(q_2, \phi)$ tele-driving. The WMR travels around two obstacles in an '8' figure shape, see fig. 5.5, with randomly varying delay 0.25∼0.35sec and 1∼2sec (Fig. 5.6 and 5.7 respectively). The WMR first travels forward to the top of the '8' figure and travels backward to the starting point. As predicted in Th. 3.1 1) the tele-operation is stable, even with round-trip

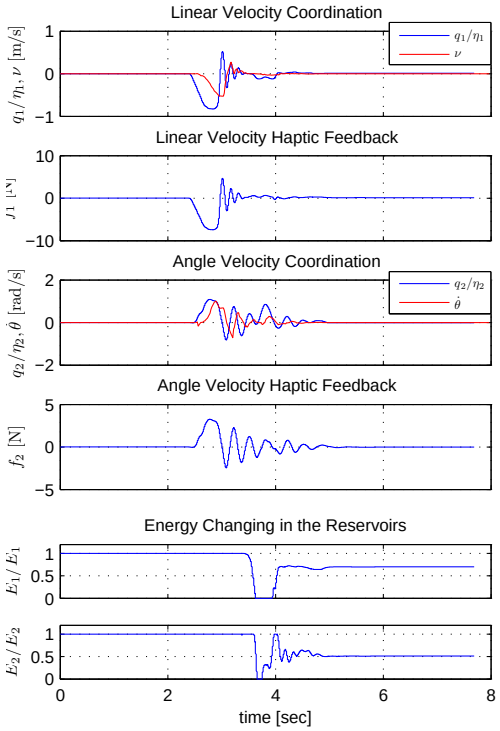

Figure 5.3: Stable case: dynamic WMR $(q_1, \nu)/(q_2, \dot{\phi})$ tele-driving with 0.25∼0.35sec randomly varying delay

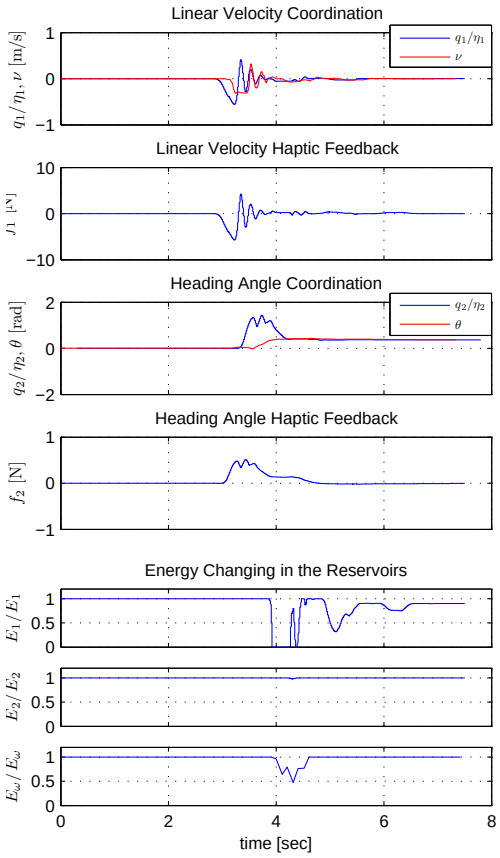

Figure 5.4: Stable case: kinematic WMR $(q_1, \nu)/(q_2, \dot{\phi})$ tele-driving with 0.25∼0.35sec randomly varying delay

1∼2sec randomly varying delay 2) linear velocity (ν) follows after the haptic device configuration q_1; 3) people can perceive the linear velocity ν via the local spring k_0; and 4) (q_2, ϕ) coordination is achieved after operator releasing the device(e.g. after 50sec in Fig. 5.7). Note that the tracking error in (q_1, ν) coordination (e.g. 5-15sec in Fig. 5.6) is due to the friction pointing backward, and that the communication delay causes bumps for f_1 (e.g. around 4sec in Fig. 5.6), and for f_2 (around 48sec in Fig. 5.7).

In Fig. 5.8, the operator commands the WMR to move toward the wall with a moderate constant q_1. The WMR measures distance from the wall using sonar sensors and stops in front of the wall (around 11sec), then after the operator releasing the device, the WMR is bounced back (after 16sec). The operator can feel the approach

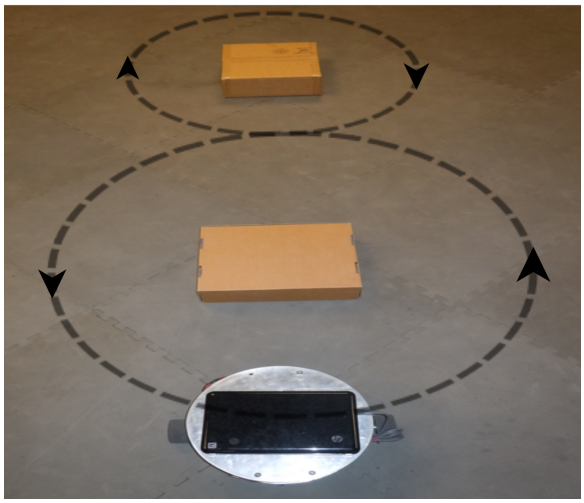

Figure 5.5: Travel around two obstacles in an '8' figure shape

of obstacles via f_1, which jumps (around 13sec) while q_1 being kept still. Besides, the third subplot shows the energy changing in the energy reservoir E_1. Note that some energy in the local spring flows to the reservoir after haptic device being released (15-20sec).

For dynamic WMR $(q_1, \nu)/(q_2, \dot{\phi})$ tele-driving, the WMR shows a similar performance (see Fig. 5.9, Fig. 5.10) except that here q_2 and $\dot{\phi}$ are coordinated. Also the operator can perceive the angular velocity via the local spring. Note when operator tele-drives WMR in $(q_1, \nu)/(q_2, \dot{\phi})$ mode, operator tries to keep WMR running forward, while tele-driving WMR in $(q_1, \nu)/(q_2, \phi)$ mode, if the heading angle is large, command WMR to turn around and run backward would become more convenient (e.g. Fig. 5.6).

In another experiment, shown in Fig. 5.11, we try to drive the WMR along the wall toward a corner with moderate q_1 and q_2, due to the virtual force/torque produced from the wall, the WMR flees away from the corner (around 9-14sec) even with q_2 being kept still, and the operator can feel the increase and decrease in the resistant force/torque (around 12-17sec). Also the last two subplots show the energy changing in reservoir E_1 and E_2.

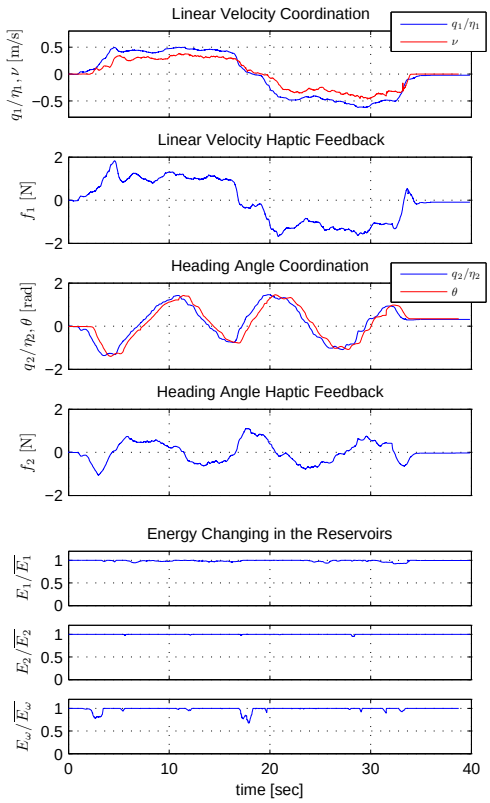

Figure 5.6: Dynamic WMR $(q_1, \nu)/(q_2, \phi)$ tele-driving with 0.25-0.35sec randomly varying delay. Average packet-to- packet interval 25.13ms for the haptic device, and 29.63ms for the WMR

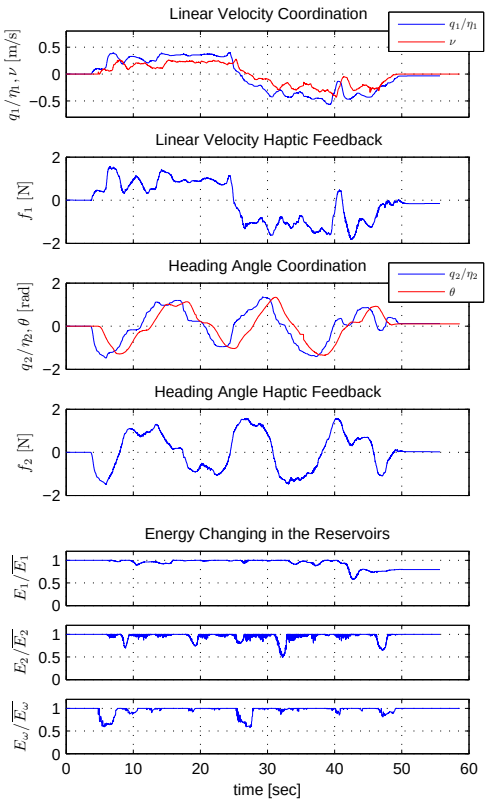

Figure 5.7: Dynamic WMR $(q_1, \nu)/(q_2, \phi)$ tele-driving with 1-2sec randomly varying delay. Average packet-to- packet interval 50.77ms for the haptic device, and 92.46ms for the WMR

Shown in Fig. 5.12 and Fig. 5.13 are the experimental results for the kinematic WMR $(q_1, \nu)/(q_2, \phi)$ tele-driving. As predicted in Th. 3.3: 1) the system shows a stable behavior; 2) the operator have velocity perception via the local spring k_0; and 3) the coordination of (q_2, ϕ) is achieved after the operator releasing the device (e.g. after 43sec in Fig. 5.12). Note the haptic feedback f_2 caused by the tracking error (e.g. 15-20sec in Fig. 5.13) serves as a helpful indicator of the (q_2, ϕ) coordinating process. Note that there are lots of oscillation of q_1 or q_2 in Fig. 5.15. This is due to the operator's overcompensation when trying to maintain the WMR on the right routine.

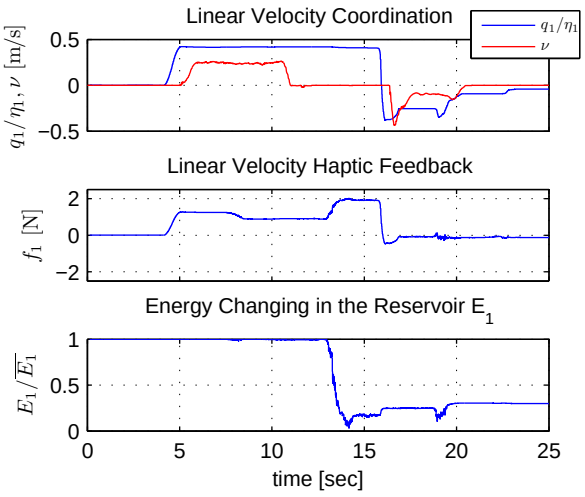

Figure 5.8: Dynamic WMR $(q_1, \nu)/(q_2, \phi)$ hard contact

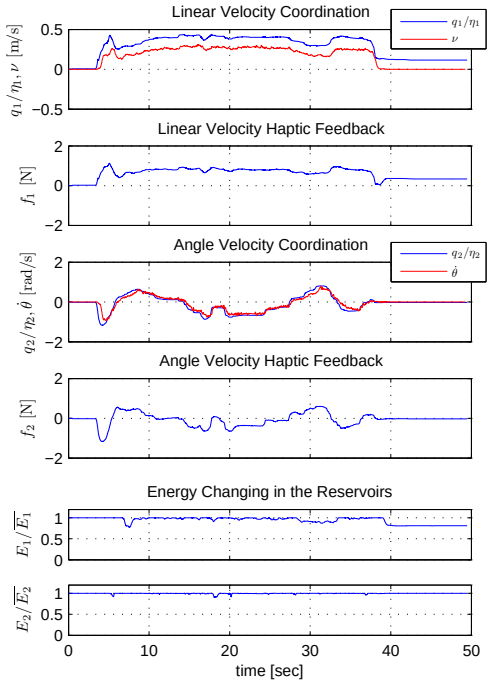

Figure 5.9: Dynamic WMR $(q_1, \nu)/(q_2, \dot{\phi})$ tele-driving with 0.25-0.35sec randomly varying delay. Average packet-to- packet interval 25.49ms for the haptic device, and 30.32ms for the WMR

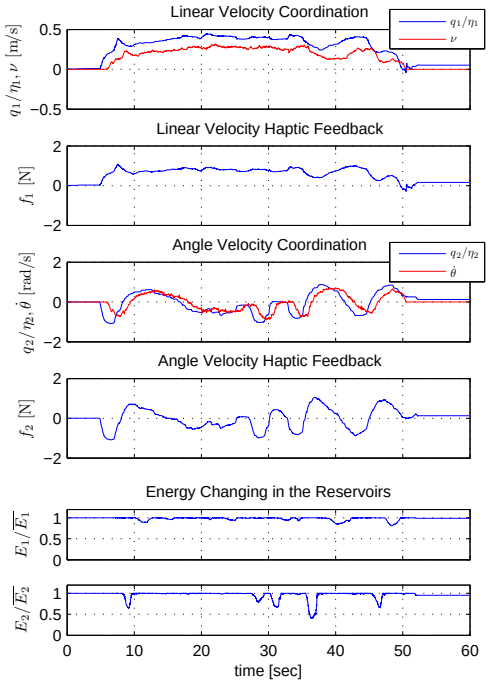

Figure 5.10: Dynamic WMR $(q_1, \nu)/(q_2, \dot{\phi})$ tele-driving with 1-2sec randomly varying delay. Average packet-to- packet interval 49.31ms for the haptic device, and 86.78ms for the WMR

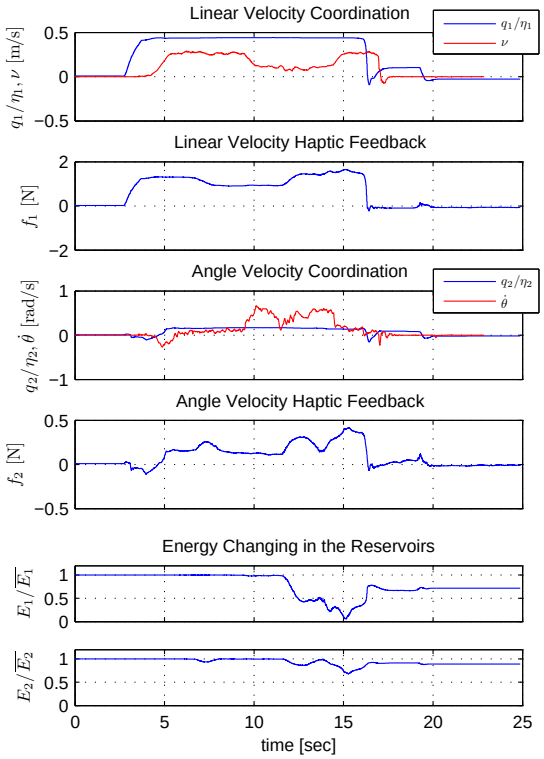

Figure 5.11: Flee Away from the Corner, for dynamic WMR $(q_1; \nu) = (q_2; \dot{\phi})$: running into a corner (around 9 sec), q2 is kept, but the WMR steers clear of the obstacle (during 9-14 sec)

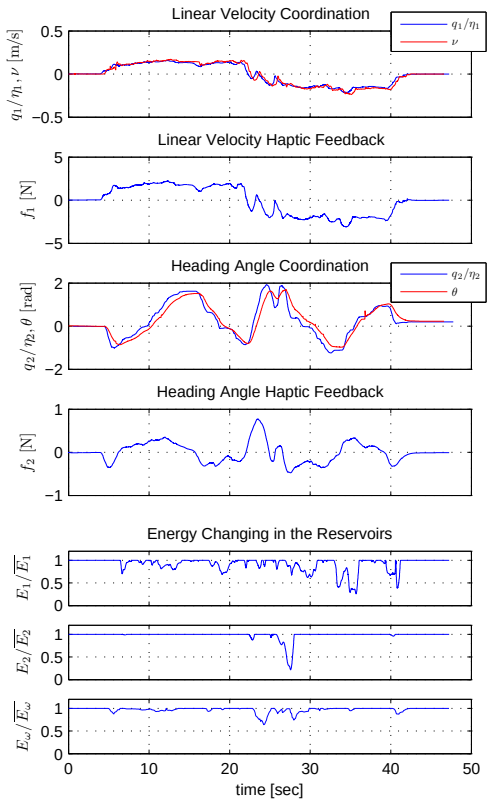

Figure 5.12: Kinematic WMR $(q_1, \nu)/(q_2, \phi)$ tele-driving with 0.25-0.35sec randomly varying delay. Average packet-to- packet interval 24.72ms for the haptic device, and 28.95ms for the WMR

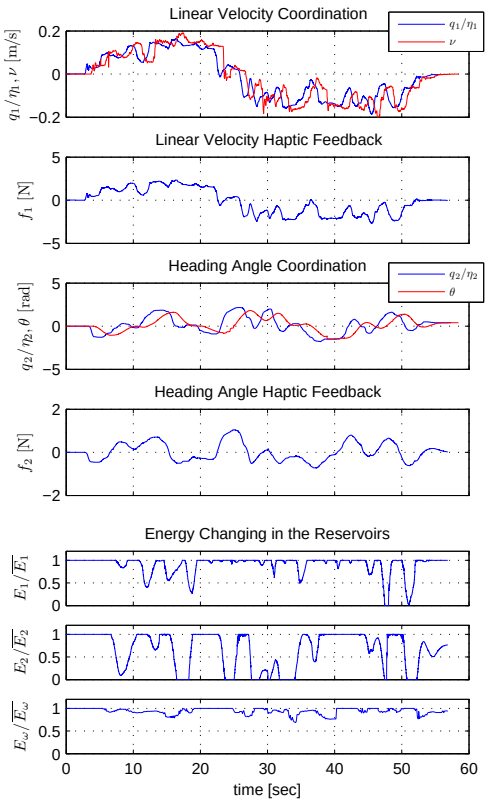

Figure 5.13: Kinematic WMR $(q_1, \nu)/(q_2, \phi)$ tele-driving with 1-2sec randomly varying delay. Average packet-to- packet interval 50.44ms for the haptic device, and 86.43ms for the WMR

In the last two Fig. 5.14 and Fig. 5.15, we use the control law in Th. 3.4 to tele-drive the kinematic WMR, both velocity $(\nu, \dot{\phi})$ and haptic feedback (f_1, f_2) follow tightly after $(q1, q2)$. And also when the delay is high, people spent more time to finish the task.

5.2 UAV haptic tele-operation

For UAV haptic teleoperation, we also use Phantom hapitc device (from Sensable, update rate 1kHz as the master device, and a Hummingbird quadrotor (from Ascending Technologies) as the slave robot. A regular PC (from Dell) with 1.86GHz

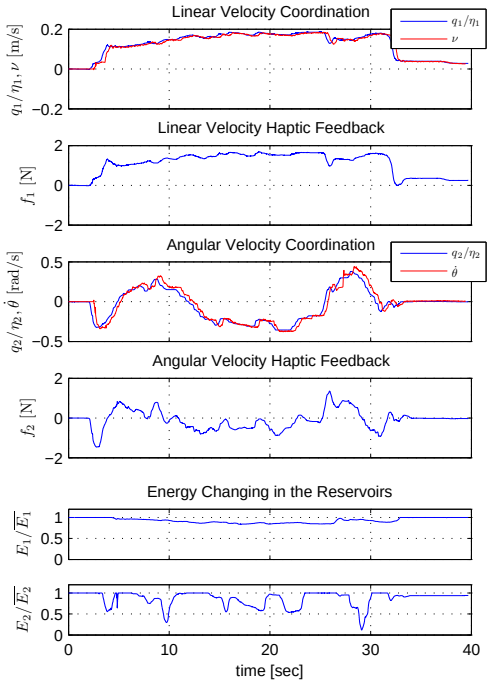

Figure 5.14: Kinematic WMR $(q_1, \nu)/(q_2, \dot{\phi})$ tele-driving with 0.25-0.35sec randomly varying delay. Average packet-to- packet interval 23.60ms for the haptic device, and 19.39ms for the WMR

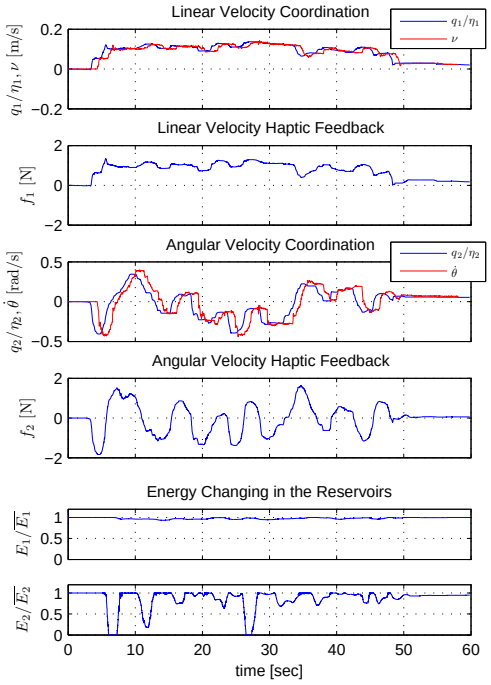

Figure 5.15: Kinematic WMR $(q_1, \nu)/(q_2, \dot{\phi})$ tele-driving with 1-2sec randomly varying delay. Average packet-to- packet interval 51.14ms for the haptic device, and 18.38ms for the WMR

CPU and 2G memory is used as the server of the system. On the PC we run the backstepping controller (update rate 50Hz) and simulate the virtual environment (update rate 100Hz). The PC and UAV are connected through a Bluetooth communication, and PC sends command at the rate of 50Hz, the same as the backstepping controller update rate. A Vicon Vision Tracking System (from Vicon) is running at 100Hz (limited by the computation capability of the computer) with a latency of 200ms (also limited by the PC) to capture the motion of the UAV. From our control frame work the backstepping controller and the virtual environment is running on the slave side. Here, for experimental purpose, they are both running on the local PC, yet we use some data buffers to created delays as if the backstepping controller and virtual environment is on the remote side.

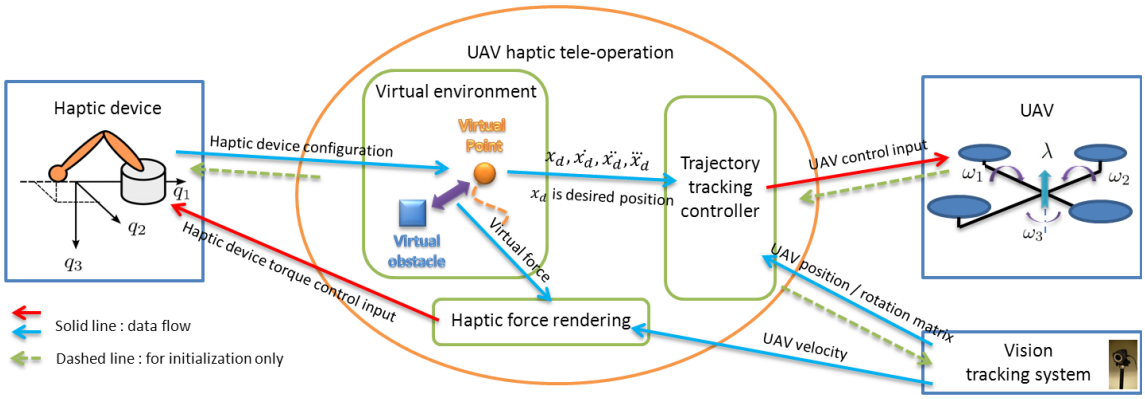

Figure 5.16: Context diagram for the UAV haptic teleoperation program

To implement the above controller, I wrote the multithread C++ program on Windows. The program runs the trajectory tracking controller, simulates the virtual environment, rendering haptic force and regulates the data flow between PC, haptic device, vision tracking system and UAV. This is illustrated in the following context diagram Fig. 5.16.

First, we test our backstepping controller and try to let the UAV travel autonomously along a predefined "8" figure shape. The UAV starts from hovering state and tries to follow the trajectory after 0sec. As shown in the Fig. 5.17, the trajectory tracking is achieved with a low tracking error $||x - x_d||$.

Then we teleoperate the UAV fly towards a virtual obstacle placed at $x = [0; 1.5; 0]$, which is marked by an actual box. The virtual point is prohibited from entering the virtual obstacle which in turn prohibits the UAV from running into the actual box. As we can see from Fig. 5.18, the UAV follows the desired trajectory well at the beginning, and operator can perceive the velocity of the UAV (from 0-7sec). As the UAV approaches the obstacle at around 7sec, the force feedback along x_2 direction suddenly increases, which give the operator clear perception of the emergence of environment obstacle. After 12sec, when the UAV flies out of the range of virtual force, we can see the human operator is able to perceive the velocity of the UAV again.

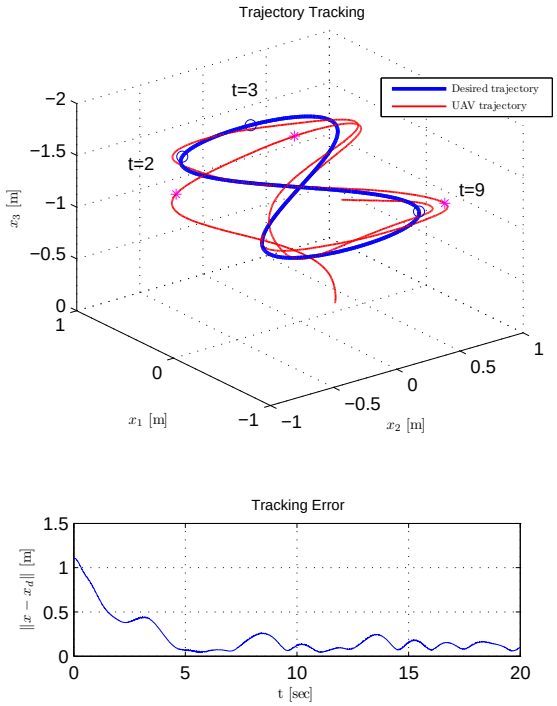

Figure 5.17: UAV trajectory tracking along a predefined "8" figure shape. The trajectory in this case is $x_d = [0.5\cos(0.2\pi t); 0.5\sin(0.4\pi t); 1.2 - 0.5\cos(0.2\pi t)$

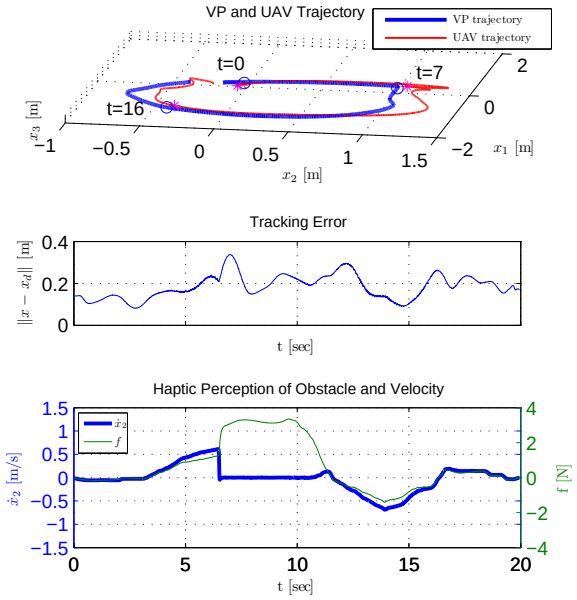

Figure 5.18: UAV haptic teleoperation over the Internet with randomly varying delay $0.25sec - 0.35sec$

Chapter 6

Conclusions

In the thesis, we study the controller design for the wheeled mobile robot(WMR) and unmanned aerial vehicle(UAV) haptic teleoperation over the Internet. Both dynamic/kinematic WMR are considered and a kind of thrust propelled UAV is considered. We extend the recently proposed passive-set-position-modulation to settle the problem of instability induced by the varying-delay and packet-loss in the communication. For UAV teleoperation we also derive a backstepping trajectory tracking control with robustness analysis. Experiments for WMRs and UAV haptic teleoperation over the Internet are shown to prove the efficacy of the control framework. This thesis would serve as a good guide for controller design for the mobile robot haptic teleoperation.

Bibliography

Bibliography

Aguiar, A. and Hespanha, J. (2007). Trajectory-tracking and path-following of underactuated autonomous vehicles with parametric modeling uncertainty. *Automatic Control, IEEE Transactions on*, 52(8):1362–1379. 6, 30

Anderson, R. and Spong, M. (1989a). Bilateral control of teleoperators with time delay. *Automatic Control, IEEE Transactions on*, 34(5):494–501. 2

Anderson, R. and Spong, M. (1989b). Bilateral control of teleoperators with time delay. *IEEE Transactions on Automatic Control*, 34(5):494–501. 5

Baiden, G. and Bissiri, Y. (2007). High bandwidth optical networking for underwater untethered telerobotic operation. In *OCEANS 2007*, pages 1–9. 1

Berestesky, P., Chopra, N., and Spong, M. (2004a). Discrete time passivity in bilateral teleoperation over the internet. In *Robotics and Automation, 2004. Proceedings. ICRA'04. 2004 IEEE International Conference on*, volume 5, pages 4557–4564. IEEE. 2

Berestesky, P., Chopra, N., and Spong, M. (2004b). Discrete time passivity in bilateral teleoperation over the internet. In *Proc. IEEE Int. Conf. Robot. Autom.*, pages 4557 – 4564. 5

Blthoff, D. L. A. F. P. R. H. I. S. H. H. (2010). Haptic Teleoperation of Multiple Unmanned Aerial Vehicles over the Internet. In *Robotics and Automation (ICRA), 2011 IEEE International Conference on*, page To appear. 3

Bouabdallah, S. and Siegwart, R. (2005). Backstepping and sliding-mode techniques applied to an indoor micro quadrotor. In *Robotics and Automation, 2005. ICRA 2005. Proceedings of the 2005 IEEE International Conference on*, pages 2247–2252. IEEE. 6

Castillo, P., Dzul, A., and Lozano, R. (2004). Real-time stabilization and tracking of a four-rotor mini rotorcraft. *Control Systems Technology, IEEE Transactions on*, 12(4):510–516. 6

Cho, S. K., Jin, H. Z., Lee, J. M., and Yao, B. (2010). Teleoperation of a mobile robot using a force-reflection joystick with sensing mechanism of rotating magnetic field. *Mechatronics, IEEE/ASME Transactions on*, 15(1):17 –26. 1

Chopra, N., Spong, M., Hirche, S., and Buss, M. (2003). Bilateral teleoperation over the internet: the time varying delay problem. In *American Control Conference, 2003. Proceedings of the 2003*, volume 1, pages 155 – 160. 2

Diolaiti, N. and Melchiorri, C. (2002). Teleoperation of a mobile robot through haptic feedback. *IEEE HAVE*, pages 67–72. 3, 4, 14

Elhajj, I., Xi, N., Fung, W., Liu, Y., Li, W., Kaga, T., and Fukuda, T. (2001). Haptic information in internet-based teleoperation. *IEEE/ASME Transactions on Mechatronics*, 6(3):295–304. 3, 40

Frazzoli, E., Dahleh, M., and Feron, E. (2000). Trajectory tracking control design for autonomous helicopters using a backstepping algorithm. In *American Control Conference, 2000. Proceedings of the 2000*, volume 6, pages 4102–4107. IEEE. 6, 29

Hannaford, B. and Ryu, J. (2002). Time-domain passivity control of haptic interfaces. *Robotics and Automation, IEEE Transactions on*, 18(1):1–10. 2

Hirche, S. and Buss, M. (2004). Packet loss effects in passive telepresence systems. In *Decision and Control, 2004. CDC. 43rd IEEE Conference on*, volume 4, pages 4010–4015. IEEE. 2

Horn, R. and Johnson, C. (2005). *Matrix analysis*. Cambridge university press. 32

Hua, M., Hamel, T., Morin, P., and Samson, C. (2009). A control approach for thrust-propelled underactuated vehicles and its application to vtol drones. *Automatic Control, IEEE Transactions on*, 54(8):1837–1853. 6, 26

Ji, M. and Egerstedt, M. (2005). Connectedness preserving distributed coordination control over dynamic graphs. In *Proceedings of the American Control Conference*, volume 1, page 93. 36

Khalil, H. K. (1996). *Nonlinear systems*. Prentice hall Englewood Cliffs, NJ, 2nd ed. edition. 7, 17, 32

Lam, T., Boschloo, H., Mulder, M., and Van Paassen, M. (2009). Artificial force field for haptic feedback in UAV teleoperation. *Systems, Man and Cybernetics, Part A: Systems and Humans, IEEE Transactions on*, 39(6):1316–1330. 3

Lamb, H. (1895). *Hydrodynamics*. Cambridge University Press, Cambridge, UK. 1

Lawrence, D. (1993). Stability and transparency in bilateral teleoperation. *Robotics and Automation, IEEE Transactions on*, 9(5):624–637. 2

Lee, D., Martinez-Palafox, O., and Spong, M. (2006a). Bilateral teleoperation of a wheeled mobile robot over delayed communication network. In *Robotics and Automation, 2006. ICRA 2006. Proceedings 2006 IEEE International Conference on*, pages 3298–3303. IEEE. 2, 34

Lee, D. and Spong, M. (2006a). Passive bilateral teleoperation with constant time delay. *Robotics, IEEE Transactions on*, 22(2):269–281. 2, 3

Lee, D. J. (2007). Passivity-based switching control for stabilization of wheeled mobile robots. In *Proc. Robot.: Sci. Sys.*, pages 70 –71. 12

Lee, D. J. (2008). Semi-autonomous teleoperation of multiple wheeled mobile robots over the internet. In *ASME Dynamic Systems & Control Conference*. 5, 6, 14, 15, 18, 19

Lee, D. J. and Huang, K. (2008). Passive position feedback over packet-switching communication network with varying-delay and packet-loss. In *Proc. HAPTICS*, pages 335–342. 5

Lee, D. J. and Huang, K. (2009a). Passive set-position modulation approach for haptics with slow, variable, and asynchronous update. In *Proc. HAPTICS*, pages 541–546. 5

Lee, D. J. and Huang, K. (2009b). Passive-set-position-modulation framework for interactive robotic systems. *IEEE Transactions on Robotics*, 26(2):354 –369. 2, 5, 16, 25, 38

Lee, D. J. and Li, P. Y. (2003). Passive bilateral feedforward control of linear dynamically similar teleoperated manipulators. *IEEE Transactions on Robotics and Automation*, 19(3):443–456. 14

Lee, D. J. and Li, P. Y. (2005). Passive bilateral control and tool dynamics rendering for nonlinear mechanical teleoperators. *IEEE Transactions on Robotics*, 21(5):936–951. 14

Lee, D. J., Martinez-Palafox, O., and Spong, M. W. (2006b). Bilateral teleoperation of a wheeled mobile robot over delayed communication network. In *Proc. IEEE ICRA*, pages 3298–3303. 2, 3, 4, 14

Lee, D. J. and Spong, M. W. (2006b). Passive bilateral teleoperation with constant time delay. *IEEE Transactions on Robotics*, 22(2):269–281. 6

Lee, S., Sukhatme, G., Kim, G., and Park, C. (2002). Haptic control of a mobile robot: A user study. In *Proc. IEEE/RSJ IROS*, pages 2867–2874. 3, 4, 14

Leung, G., Francis, B., and Apkarian, J. (1995). Bilateral controller for teleoperators with time delay via μ-synthesis. *Robotics and Automation, IEEE Transactions on*, 11(1):105–116. 2

Lim, J., Ko, J., and Lee, J. (2003). Internet-based teleoperation of a mobile robot with force-reflection. In *Proc. IEEE CCA*, pages 680–685. 1, 3

Mahony, R. and Hamel, T. (2004). Robust trajectory tracking for a scale model autonomous helicopter. *International Journal of Robust and Nonlinear Control*, 14(12):1035–1059. 6

Niemeyer, G. and Slotine, J. (1991). Stable adaptive teleoperation. *Oceanic Engineering, IEEE Journal of*, 16(1):152–162. 2

Niemeyer, G. and Slotine, J. (1998). Towards force-reflecting teleoperation over the internet. In *Robotics and Automation, 1998. Proceedings. 1998 IEEE International Conference on*, volume 3, pages 1909–1915. IEEE. 2

Niemeyer, G. and Slotine, J. (2004). Telemanipulation with time delays. *International Journal of Robotics Research*, 23(9):873–890. 6

Nourbakhsh, I., Sycara, K., Koes, M., Yong, M., Lewis, M., and Burion, S. (2005). Human-robot teaming for search and rescue. *IEEE Pervasive Computing*, pages 72–78. 1

Nuño, E., Basañez, L., Ortega, R., and Spong, M. (2009a). Position tracking for non-linear teleoperators with variable time delay. *The International Journal of Robotics Research*, 28(7):895. 2

Nuño, E., Basañez, L., Ortega, R., and Spong, M. (2009b). Position tracking for non-linear teleoperators with variable time delay. *The International Journal of Robotics Research*, 28(7):895. 5

Peshkin, M. and Colgate, J. (1999). Cobots. *Industrial Robot*, 26(5):33–34. 1

Rodríguez-Seda, E., Troy, J., Erignac, C., Murray, P., Stipanovic, D., and Spong, M. (2010). Bilateral teleoperation of multiple mobile agents: coordinated motion and collision avoidance. *Control Systems Technology, IEEE Transactions on*, 18(4):984–992. 3

Salcudean, S., Zhu, M., Zhu, W., and Hashtrudi-Zaad, K. (2000). Transparent bilateral teleoperation under position and rate control. *The International Journal of Robotics Research*, 19(12):1185. 2

Schenker, P., Huntsberger, T., Pirjanian, P., Baumgartner, E., and Tunstel, E. (2003). Planetary rover developments supporting mars exploration, sample return and future human-robotic colonization. *Autonomous Robots*, 14(2):103–126. 1

Slawinski, E., Mut, V., and Postigo, J. (2007). Teleoperation of mobile robots with time-varying delay. *IEEE Transactions on Robotics*, 23(5):1071–1082. 3

Stramigioli, S., Mahony, R., and Corke, P. (2010). A novel approach to haptic teleoperation of aerial robot vehicles. In *Robotics and Automation (ICRA), 2010 IEEE International Conference on*, pages 5302–5308. IEEE. 3

Valavanis, K. (2007). *Advances in unmanned aerial vehicles: state of the art and the road to autonomy*. Springer Verlag. 1

Zuo, Z. and Lee, D. J. (2010). Haptic Tele-Driving of a Wheeled Mobile Robot over the Internet: a PSPM Approach. In *Proc. IEEE CDC*, pages 3614–3619. 1

Zuo, Z. and Lee, D. J. (2011). Backstepping Control of Quadrotor-type UAVs: Trajectory Tracking and Teleoperation over the Internet. In *To submit*. 1

Vita

Zhiyuan Zuo was born in 1987, Shandong, China. He received his bachelor's degree in 2009, Harbin Institute of Technology in Automotive Engineering. He joined robotics laboratory since sophomore year and worked hard there trying to be a good engineer. After college, he came to US for further study in Robotics and control. In graduation study, he worked as a research assistant in INRoL, UTK and also as a teaching assistant in Mechatronics lab class. He would begin his career as an engineer after graduation.